UNIVERSITAT DE BARCELONA

Departament de Fisiologia
Facultat de Farmàcia

ADAPTACIONS DEL CÒLON DE RATA AL CONTINGUT EN SODI DE LA DIETA: PAPER DEL SISTEMA RENINA-ANGIOTENSINA-ALDOSTERONA I DE LA VASOPRESSINA

Esther Cristià Civit

2006

PAPERS
ARTICLES

01.

PAPER DE L'ALDOSTERONA I DE L'ANGIOTENSINA II EN LA PERMEABILITAT DEL COLON DISTAL

ALDOSTERONE REDUCES CRYPT COLON PERMEABILITY DURING LOW-SODIUM ADAPTATION

M. Moretó, E. Cristià, A. Pérez-Bosque, I. Afzal, C. Amat, R.J. Naftalin

Journal of Membrane Biology 206: 43-51, 2005

Els resultats del present article s'han presentat a les següents comunicacions:

The results of the present paper have been presented in the following communications:

Moretó M, Amat C, Cristià E, Pérez-Bosque A, Villà C, Afzal I, Naftalin RJ
Effects of high and low Na+ diets on colonia crypt function in adrenalectomized rats

Seleccionat com a comunicació oral en el congrés:

19th European Intestinal Transport Group Meeting
Guilford, UK, 17-20 Abril 2004

Publicat a J Physiol Biochem 60:143, 2004

Selected as an oral communication in the meeting:

19th European Intestinal Transport Group Meeting
Guilford, UK, 17-20 April 2004

Published in J Physiol Biochem 60:143, 2004

Cristià E, Afzal I, Pérez-Bosque A, Amat C, Moretó M, Naftalin RJ
Role of aldosterone and angiotensin II in rat colon functions during the transition from high sodium to low sodium diet

Presentat com a pòster en el congrés:

XXXIII Congreso de la Sociedad Española de Ciencias Fisiológicas (SECF). Sevilla, 10-13 Febrer 2005

Publicat a J Physiol Biochem 61:189, 2005
Premi a un dels millors pòsters del congrés.

Presented as a poster in the meeting:

XXXIII Congreso de la Sociedad Española de Ciencias Fisiológicas (SECF). Sevilla, 10-13 Feb 2005

Published in J Physiol Biochem 61:189, 2005 Awarded as one of the best poster in the congress

RESUM ARTICLE 1

Introducció: El còlon distal participa en la resposta homeostàtica electrolítica de l'organisme. Degut a una disminució en la ingesta de sodi, es produeixen canvis en la permeabilitat del còlon, els quals no està clar si són deguts a l'acció de l'aldosterona, de l'angiotensina II o a l'acció sinèrgica d'ambdues hormones, ja que una dieta amb baix contingut en sodi activa el sistema renina-angiotensina-aldosterona que acaba donant lloc a un augment de la concentració plasmàtica tant d'angiotensina II com d'aldosterona.

Objectius: Reproduir els canvis en la permeabilitat del còlon distal que es produeixen en la transició d'una dieta amb alt contingut en dosi (HS) a tres dies d'una dieta amb baix contingut en sodi (LS). Determinar el paper de l'aldosterona i l'angiotensina II per separat en aquesta adaptació del còlon distal.

Material i Mètodes: Rates mascles Sprague-Dawley de 250 g de pes aproximat s'han alimentat amb dietes HS o LS. A rates d'ambdues dietes se'ls ha realitzat una adrenalectomia i se'ls ha administrat aldosterona, angiotensina II o vehicle mitjançant bombes osmòtiques per via subcutània. A més de fer un seguiment de les variables fisiològiques, s'ha estudiat el flux de sodi des de l'exterior de les criptes a l'espai pericriptal, la permeabilitat a macromolècules de les criptes de còlon distal de rata emprant dextrà 10 kDa com a traçador i l'expressió del canal epitelial de sodi, ENaC, en els colonòcits mitjançant imunohistoquímica i la posterior obtenció de les imatges mitjançant microscopia confocal. També s'han realitzat estudis d'electrofisiologia, determinant la diferència de potencial, el corrent de curt-circuit, i la resistència transepitelial.

Resultats: L'adaptació a una dieta LS al còlon distal comporta una disminució de la permeabilitat de la paret de la cripta al dextrà i un increment en la resistència elèctrica. A més, també s'observa un increment de la concentració de sodi a l'espai pericriptal i en l'expressió de γ-ENaC en els colonòcits. Independentment de la dieta, l'administració d'aldosterona a animals adrenalectomitzats reprodueix els efectes de la dieta LS, disminuint la permeabilitat al dextrà, incrementant la resistència del teixit, incrementant l'acumulació de sodi en la zona pericriptal i augmentant l'expressió del canal de sodi. En canvi, l'administració d'angiotensina II a animals amb una concentració plasmàtica d'aldosterona mínima, no dóna lloc a aquests canvis, mostrant uns resultats semblants al grup d'animals alimentats amb una dieta HS.

Conclusió: Una disminució en la ingesta de sodi produeix adaptacions funcionals en el còlon distal de rata facilitant el transport electrogènic de sodi i la seva acumulació a la zona pericriptal i augmentant la resistència de l'epiteli. L'aldosterona té un paper clau en els canvis que afecten la permeabilitat en el còlon distal deguts a una dieta amb baix contingut en sodi. L'angiotensina II no sembla tenir un paper rellevant i no actua de manera sinèrgica amb l'aldosterona.

J. Membrane Biol. 206, 43–51 (2005)
DOI: 10.1007/s00232-005-0772-5

The Journal of
Membrane
Biology

Aldosterone Reduces Crypt Colon Permeability during Low-Sodium Adaptation

M. Moretó[1], E. Cristià[1], A. Pérez-Bosque[1], I. Afzal-Ahmed[2], C. Amat[1], R.J. Naftalin[2]
[1]Departament de Fisiologia, Facultat de Farmàcia, Universitat de Barcelona, Barcelona, Spain
[2]Physiology Division, King's College London, Guys Campus, London, UK

Received: 26 August 2005

Abstract. Fluid and electrolyte absorption by colonic crypts depends on the transport properties of crypt cellular and paracellular routes and of the pericryptal sheath. As a low-Na^+ diet increases aldosterone and angiotensin II secretion, either hormone could affect absorption. Control and adrenalectomized (ADX) Sprague-Dawley rats were kept at a high-NaCl (HS) diet and then switched to low-NaCl (LS) diet for 3 days. Aldosterone or angiotensin II plasma concentrations were maintained using implanted osmotic mini-pumps. The extracellular Na^+ concentration in isolated rat distal colonic mucosa was determined by confocal microscopy using a low-affinity Na^+-sensitive fluorescent dye (Sodium red, and Na^+-insensitive BODIPY) bound to polystyrene beads. Crypt permeability to FITC-labelled dextran (10 kDa) was monitored by its rate of escape from the crypt lumen into the pericryptal space. Mucosal ion permeability was estimated by transepithelial electrical resistance (TER) and amiloride-sensitive short-circuit current (SCC). The epithelial Na^+ channel, ENaC, was determined by immunolocalization. LS diet decreased crypt wall permeability to dextran by 10-fold and doubled TER. Following ADX, aldosterone decreased crypt wall dextran permeability, increased TER, increased Na^+ accumulation in the pericryptal sheath and ENaC expression even in HS. Infusion of angiotensin II to ADX rats did not reverse the effects of aldosterone deprivation. These findings indicate that aldosterone alone is responsible for both the increase in Na^+ absorption and the decreased paracellular and pericryptal sheath permeability.

Key words: Aldosterone — Angiotensin II — Colon — Permeability

Correspondence to: M.Moretó; email: mmoreto@ub.edu

Introduction

The major function of rat and human distal colon is absorption of NaCl and water. Aldosterone is thought to be the key hormone in the regulation of Na^+ homeostasis, however, colonic absorptive function depends not only on active Na^+ transport across crypt luminal cells, but also on the myofibroblast cells of the surrounding pericryptal sheath. This matrix generates a barrier to macromolecules and NaCl diffusion, thereby promoting and maintaining NaCl accumulation within the space lying between the colonocytes and the sheath. This hypertonic "central" compartment generates an osmotic gradient across the cells between the crypt lumen and pericryptal space and a hydrostatic pressure gradient across the sheath, which forces fluid outflow into the interstitial space outside the sheath (Naftalin & Pedley, 1999).

Colonic Na^+ absorption is influenced by a low-sodium diet. Low NaCl concentrations at the macula densa segment of the renal distal tubule increase renin secretion into the blood, thereby activating the renin-angiotensin-aldosterone system (RAAS). Renin cleaves angiotensinogen secreted by the liver to angiotensin I. Angiotensin I is then cleaved by angiotensin-converting enzyme (ACE) to angiotensin II (ANG II). Thereafter, ANG II increases aldosterone (ALDO) secretion by stimulating its synthesis in the adrenal zona glomerulosa (Peart, 1969). In addition to this classical pathway of ANG II synthesis, tissue RAAS have been identified in a number of organs, suggesting that various tissues have the ability to synthesize ANG II independently of the circulating RAAS (Paul, Wagner & Dzar, 1993). Tissue-specific RAAS may be present in the kidney, brain, vasculature, adrenal, heart (Campbell & Habener, 1986) and colon (Hirasawa et al., 2002).

In rat hearts exposed to raised concentrations of ANG II and ALDO, there is proliferation of myofibroblasts and an increase of collagen (Campbell,

Janieki & Weber, 1995). So, apparently, both angiotensin II and aldosterone have roles in inducing cardiac fibrosis. Colonic mucosal fibrosis is induced as a chronic reaction to radiation and can be reversed by long-term treatment with the ACE inhibitor captopril (Thiagarajah et al., 2002). Fibrosis in lung, kidney, heart and brain following radiation or as a consequence of chronic inflammation have also been described and are ameliorated by ACE inhibitors or angiotensin antagonists like losartan (Molteni, Moulder & Cohen, 2000; Naftalin, 2004).

As colonic absorptive function depends on crypt luminal cells and on myofibroblasts and as Na^+ depletion upregulates both ALDO and ANG II secretion, it is important to delineate the role of each hormone in each component of colonic permeability. The aim here is to investigate the separate roles of aldosterone and angiotensin II in the structural and functional adaptations of the colon in response to changes in dietary Na^+ intake.

Materials and Methods

Experimental Animals

Studies were performed on adult male Sprague-Dawley rats (Harlan Iberica, Barcelona, Spain) weighing 200–250 g the day of experiment. They were housed one per cage under 12:12 h light-dark cycle and food and water were available *ad libitum*. Experimental procedures were approved by the Ethical Committee for Animal Experimentation of the Universitat de Barcelona.

Experimental Protocols

Protocol 1: Experimental Protocol for Examining Effect of Diets and Pharmacological Treatment

Animals received a high-sodium diet (HS, wheat and barley plus 150 mM NaCl in drinking water). After 4 days the diet of some animals was altered to a low-sodium diet (LS, wheat and barley and drinking water containing 150 μM NaCl) for 3 days. In preliminary studies the rats were fed a LS diet for 1, 3, 5 and 7 days. These results showed that there were significant effects after 3 days, so the subsequent experiments were done only using the 3-day time period. Groups of rats received the angiotensin converting enzyme (ACE) inhibitor, captopril (CAP) or the angiotensin II receptor type 1 (AT1) inhibitor, losartan (LOS), or the aldosterone antagonist, spironolactone (SPI). Captopril and losartan were administered in drinking water at a dose of 65 mg/kg·day and 30 mg/kg·day, respectively, and spironolactone (10 mg/kg·day) was given by gavage, suspended in water containing 25% propylene glycol.

Protocol 2: Experimental Protocol of ADX Followed by Hormonal Replacement

Some rats were anesthetized with isofluorane (Inibsa®, Spain) and were adrenalectomized (ADX) via bilateral flank incisions. At the time of ADX, osmotic minipumps (model 2002, Alzet, Palo Alto, CA) were implanted subcutaneously in the neck of each rat. Two hormones were replaced using minipumps: D-aldosterone (Sigma) dissolved in propylene glycol, was delivered at a rate of 450 μg/kg day (ALDO groups) and angiotensin II (Sigma) dissolved in saline, was delivered at a rate of 288 μg/kg day (ANG II groups). Groups without hormonal replacement were implanted with pumps delivering vehicle alone. The pumps were equilibrated with saline overnight before insertion. Both ALDO and ANG II plasma concentrations are chronically increased with this protocol.

All ADX groups received dexamethasone with the osmotic minipumps. Dexamethasone was chosen as a representative glucocorticoid because it binds more selectively to the glucocorticoid receptor than corticosterone, the predominant endogenous glucocorticoid in the rat (Funder et al., 1973). A dexamethasone dose of 12 μg/kg day was chosen as the lowest dose necessary for maintenance of normal weight gain, glomerular filtration rate and normal fasting plasma glucose and insulin levels (Stanton et al., 1985).

After surgery the animals were kept on the HS diet during 4 days. Thereafter, half of the animals were changed to LS diet for 3 days and the other half continued with HS diet. With this protocol we obtain 6 groups with different hormonal profile: ADX·HS + ALDO, ADX·HS + ANG, ADX·HS, ADX·LS + ALDO, ADX·LS + ANG, and ADX·LS.

Tissue Preparation

Rats from both protocols were maintained in metabolic cages during the last three days, and 24-h urinary output, water intake, food consumption and weight increase were measured daily. Urinary volume, osmolality, Na^+ and K^+ concentrations, ANG II and ALDO concentrations were also measured. To prevent urinary bacterial growth, azlocillin (0.5 mg, Sigma) was added to the collection tube. Thereafter, rats were anaesthetized with ketamine/xylacine (100/10 mg/kg) i.p.; the descending colon was removed rapidly and the contents were removed by washing with PBS. Colonic mucosa was isolated from the muscularis mucosae by scraping with a glass slide and maintained in Earl's medium for its use in in vitro functional studies (pericryptal Na^+ concentration, dextran permeability), or fixed in 4% paraformaldehyde in PBS at 4°C for 24 h for immunohistochemistry studies. The tissue was washed and stored in PBS at 4°C. Trunk blood was collected in tubes containing EDTA (1.5 mg/ml of blood) and a protease inhibitor cocktail (Sigma) and kept on ice until centrifugation at 4°C. Plasma was aliquoted and stored at −80°C for subsequent assay of plasma hormone and ion concentrations.

Plasma and Urinary Ion Concentration

Plasma K^+ and Na^+ concentrations were measured using potentiometric direct dry chemistry (Beckman Coulter Corporation). Their urinary concentrations were determined using inductively coupled plasma optical emission spectroscopy (ICP-OES Thermo Jarrell Ash model ICAP 61E, Genesis Laboratories Systems Inc., Colorado).

Hormone Determinations

Urine and plasma hormones were determined by RIA using commercially available kits: ALDOCTK-2, DiaSorin S.p.A. (Italy) for urinary aldosterone, Aldosterone RIA kit Immunotech for plasma aldosterone and RIA I^{125} Bühlmann Laboratories (Switzerland) for plasma angiotensin II.

Electrical Parameters

Freshly excised segments of distal colon were mounted in the Ussing chambers. The volume of the bathing solution in each chamber was 4 ml with a tissue internal surface area of 0.63 cm^2. The Krebs

bathing solution buffer contained (in mM) 115 NaCl, 25 $NaHCO_3$, 2 KH_2PO_4, 8 KCl, 1.2 $CaCl_2$, 1.1 $MgCl_2 \cdot 6H_2O$. Glucose (10 mM) was added to the buffer bathing the serosal side of the tissue, and this was osmotically balanced by addition of 10 mM mannitol to the mucosal buffer. Each solution was continuously oxygenated with 95% O_2-5% CO_2 and circulated by gas lift, pH 7.4 and 37°C. Two pairs of Ag/AgCl electrodes monitored the transmural potential difference (*PD*, mV) under open-circuit conditions or the short-circuit current (I_{sc}, $\mu A/cm^2$) with transmural *PD* clamped to zero using voltage clamp (Dipl.-Ing. K. Mussler Scientific Instruments, Aachen, Germany) connected to a PC equipped with clamp-specific software (Clamp v.2·14, Aachen, Germany). Transepithelial electrical resistance (*TER*; $ohm \cdot cm^2$) was obtained from the clamp program by constant current pulses at 15 s intervals. Experiments were carried out simultaneously in six chambers. After a 30-min equilibration period, *PD*, I_{sc} and *TER* were recorded in the basal state every 6 s under voltage-clamp conditions and after addition of apical amiloride (0.1 mM) to measure basolateral Na^+ pump activity, over a period of 1 h in Krebs.

Pericryptal Na^+ Accumulation

Na^+ concentration in isolated rat distal colonic mucosa was determined using a modification of a dual-wavelength laser scanning confocal microscopic method in which low affinity Na^+-sensitive dye (Sodium Red, and BODIPY-fl) are bound to microscopic polystyrene beads (Jayaraman et al., 2001). Fifty mg of sodium red (sample provided by Molecular Probes, Eugene, OR; catalog no. 71351) and 30 μg of BODIPY-fl in 2% methanol-water were added to a 1% (vol/vol) suspension of 50-nm-diameter carboxyl latex beads (Polymer Lab, Amherst, MA) suspended in 4 ml of water. The chromophores remained quantitatively immobilized on the beads during measurements and for > 2 months of storage in water at 4°C in the dark. Colonic mucosal pieces were loaded with the dye-containing beads with 200 μl of a 10% (vol/vol) solution by incubation for 1 h. The method used here uses smaller beads than previously (Thiagarajah et al., 2001a). This improves the rate of bead uptake into the extracellular space and makes better contrast and delineation of the extracellular Na^+ concentration. The local Na^+ concentration was estimated by ratiometric imaging of the beads using the Na^+ red signal, which increases linearly in the concentration range 0–500 mM and the green signal from BODIPY-fl.

Na^+ Ratio Analysis

Image pairs of sodium red and BODIPY-fl were acquired from the same field. Background images were obtained under the same conditions but without loading with the dye. Analysis was performed using Image J software http://rsb.info.nih.gov. Ratio images (red-to-green fluorescence) were obtained by pixel-by-pixel division of background-subtracted images. Background values were < 10% of signal. Averaged ratios were obtained by integration of red and green fluorescence intensities over specified regions of interest. Two to three crypts were measured from each set of images.

Dextran Permeability

Crypt permeability to dextran was monitored by the rate of escape of fluorescein isothiocyanate (FITC)-labeled dextran (molecular weight 10,000, FITC dextran; Sigma Chemicals, St Louis, MI) from the crypt lumen into the pericryptal space at 37°C. Crypt luminal and pericryptal concentration of FITC-dextran were estimated by monitoring the ratio of fluorescence intensity of each zone. The procedures performed were as described (Naftalin, Zammit & Pedley, 1999).

Immunocytochemistry

Colonic mucosal tissue (0.5 cm^2 pieces) was placed in 1.5 ml Eppendorf tubes and were permeabilized in 0.2% Triton X-100 in blocking buffer (1% BSA in PBS and glycine) for 30 min. Samples were washed three times in PBS and incubated for 90 min with rabbit anti-rat γ-ENaC antibody (1:100, Alpha Diagnostics Intl., San Antonio, TX), washed 3 × in PBS and then incubated for 60 min in secondary anti-rabbit Alexa-488 antibody (Molecular Probes, Eugene, OR) diluted 1:100 with PBS and washed again 3 × in PBS.

Confocal Images

Each piece of tissue was viewed from the mucosal side with the confocal microscope using a 20× or 40× Leica SPII oil immersion lens. The focus plane was taken to the surface of the tissue and images were captured at 2.5 μm or 5 μm steps using the automatic Z-step motor. Images were taken from 0 μm down to 40 μm below the surface. With dextran permeability measurements, the scans were repeated at 5 min intervals for 20 min. For Na^+-red ratio imaging, the tissues were pre-incubated at 37°C in a humidified hood for 30 min with the dye prior to viewing with the confocal microscope. This allows the dye beads to penetrate into the pericryptal and interstitial spaces. The captured images represent the general level of staining throughout the whole tissue and were obtained with the same optical conditions, gain and section size.

Image Analysis

The captured images were analyzed using the program Image J (Image J 1.32, http://rsb.info.nih.gov/ij/index.html) (Rasband, 1997–2005) to quantify the fluorescence from each antibody (Abramoff, Magelhaes & Ram, 2004). The fluorescence was quantified by areas, which were divided into either crypt or inter-crypt and were taken by selecting a region of interest within the relevant part of the image. Three areas of both crypt and inter-crypt regions were taken for image analyses and therefore there were thirty measurements per tissue at the various depths. The mean and SEM of the measurements after background subtraction from each image were calculated. To obtain averaged fluorescence intensities within the crypt lumen and pericryptal sheath, projected images using maximal intensity averaging over the depths 5–30 μm were obtained for each rat and results compared for each condition.

Statistical Analyses

Data were expressed as means ± SEM. Comparisons between HS and LS diet were made by ANOVA using SPSS-10.0 software (SPSS). To analyze the effects of pharmacological treatment, groups were compared with the LS group by ANOVA followed by Scheffe's *post-hoc* test. In ADX groups, the groups with ALDO or ANG II replacement were compared with the groups without supplementation by ANOVA followed by Scheffe's *post-hoc* test. In results of electrical parameters, the effect of amiloride was tested by ANOVA. Differences were considered statistically significant when the test yielded $P < 0.05$.

Results

Metabolic and Hormonal Changes

The physiological variables relating to body weight, food and water intake, and to urinary function,

Table 1. Functional data from rats in protocol 1

Protocol 1	Units	HS	LS 3D	LS 3D CAP	LS 3D LOS	LS 3D SPI
Weight gain (3 days)	g	7.9 ± 1.1 (7)	6.3 ± 0.6 (7)	−2 ± 1.0 (6)#	−0.8 ± 0.7 (5)#	−0.1 ± 1.6 (5)#
Food consumption (3 days)	g	63 ± 3.1 (8)	63 ± 3.8 (8)	53 ± 3.7 (5)#	52 ± 3.6 (5)*	57 ± 3.9 (5)#
Water intake (3 days)	ml	84 ± 6.3 (8)	68 ± 4.8 (8)	73.3 ± 6.7 (5)	127 ± 16.1 (5)#	138 ± 22.2 (5)#
Urine volume (3 days)	ml	35.3 ± 3.7 (8)	30.47 ± 4.2 (8)	42.2 ± 2.1 (5)#	99.7 ± 19.4 (5)#	110.7 ± 17.9 (5)#
Urinary Na^+ (3 days)	mmol	8.87 ± 0.73 (6)	0.28 ± 0.06 (7)*	0.13 ± 0.01 (4)*	0.09 ± 0.02 (4)*	0.11 ± 0.03 (4)*
Urinary K^+ (3 days)	mmol	4.28 ± 0.28 (6)	4.09 ± 0.18 (7)	3.9 ± 0.96 (4)	3.96 ± 0.51 (4)	4.41 ± 0.33 (4)
Na^+ plasma at day 3	mM	142.1 ± 1.2 (6)	143.9 ± 1.1 (6)	141.7 ± 0.7 (6)	143.7 ± 1.7 (7)	145.6 ± 0.5 (7)
K^+ plasma at day 3	mM	4.48 ± 0.31 (6)	4.23 ± 0.15 (6)	4.62 ± 0.26 (6)	4.45 ± 0.22 (7)	4.36 ± 0.14 (7)
Cl^- plasma at day 3	mM	100.1 ± 0.9 (6)	100.6 ± 0.5 (6)	98.1 ± 0.7 (6)	101.3 ± 1.5 (7)	101.9 ± 0.3 (7)
Aldosterone plasma	nM	0.63 ± 0.07 (4)	1.21 ± 0.27 (7)*	0.60 ± 0.17 (5)#	0.73 ± 0.12 (5)*	2.98 ± 0.71 (5)#
Angiotensin II plasma	pg/ml	57.8 ± 4.8 (5)	85.8 ± 9.9 (7)*	60.05 ± 3.9 (5)*	95.7 ± 8.9 (5)	141.5 ± 23.5 (5)#

Protocol 1 involves rats fed HS or LS diets and rats treated with captopril (CAP), losartan (LOS) and spironolactone (SPI). Variables with the expression "3 days" include the results obtained by summing the results of the three last days before sacrifice; the expression "at day 3" refers to variables measured during the third day in the metabolic cage. Values are means ± SEM (in parentheses, the number of animals). *$P < 0.001$ HS *vs.* LS; #$P < 0.001$ LS *vs.* pharmacological treatment.

plasma ion and hormone concentrations are shown in Tables 1 (protocol 1) and 2 (protocol 2).

Plasma concentrations of aldosterone and angiotensin II are significantly increased after 3 days in the LS diet, compared with the HS diet (Table 1). Of the six groups obtained following adrenalectomy (ADX) the two with ALDO replacement (protocol 2) have high plasma concentrations of aldosterone and the other four, very low levels, as expected (Table 2). It is worth noting that the ADX·LS + ALDO group has a low ANG II plasma concentration, suggesting that high circulating aldosterone concentrations may inhibit RAAS directly or indirectly. ANG II infusion raised the circulating concentration of this hormone in ADX·HS + ANG and ADX·LS + ANG groups (Table 2). Urinary aldosterone excretion in 3 days following dietary switch from HS to LS is raised from 51 ± 5.6 pmol to 201 ± 51.4 pmol ($n = 6$) but is negligible in the 3 days post ADX. The polydipsia and polyuria as well as K^+ depletion observed in the ADX·HS + ALDO are consistent with characteristics of the Conn's syndrome (Fardella & Mosso, 2002).

The key physiological variables relating to aldosterone function are that net Na^+ loss during 3 days with LS diet following ADX is raised without ALDO supplementation; with ALDO replacement, urinary Na^+ loss is half that seen without ALDO replacement, or with ANG II replacement (Table 2). Weight loss correlates with these findings. With an LS diet following ADX, in animals without ALDO supplement, there is net weight loss; whereas ALDO supplementation prevents weight loss. ANG II supplementation without ALDO increases weight loss (Table 2).

Another indicator of low aldosterone activity following ADX is the high plasma K^+ concentration seen without ALDO supplementation (Table 2). This shows that K^+ excretion via the urine and faeces fails to match the rise in plasma K^+ concentration. These findings indicate that the dietary, surgical and pharmacological treatments were efficacious.

Effect of HS and LS Diet and Aldo Supplementation post ADX on Rat Distal Colon Electrical Parameters

Table 3 shows that in LS conditions there are significant increases in PD, I_{sc} and *TER* compared with HS conditions ($P < 0.01$). Amiloride (0.1 mM) abolishes the *PD* and I_{sc} but does not affect the LS-dependent increase in *TER*. In ADX rats following ALDO replacement in both HS and LS there are similar increases in *PD*, I_{sc} and electrical resistance. The LS and aldosterone-dependent increases in I_{sc} and *PD* abolished by amiloride (0.1 mM) are similar to those found by many others (Fromm & Hegel, 1978; Horster et al., 1994). However the increase in *TER* is only observed by a few, some observe a decrease, whilst others find no change in *TER* (Dolman, Edmonds & Salas-Coll 1978; Schulzke, Fromm & Hegel, 1986). The large increase in *TER* observed here may relate to the time of exposure to the hormone *in vivo* prior to measurement in vitro. The concurrent effects of dextran permeability develop over 3–5 days. Much smaller effects are observed after 24 hours.

Effect of HS and LS Diet and ALDO or ANG II Supplementation post ADX on Rat Distal Colon Permeability to Dextran

The crypt wall permeability to dextran determined from the rate of escape of FITC-labeled dextran (10 kDa) from the crypt lumen into the pericryptal space was used as an index of the permeability of the pericryptal barrier (Thiagarajah et al., 2001b). During the

Table 2. Functional data from rats in protocol 2

Protocol 2	Units	ADX HS+ALDO	ADX HS+ANG	ADX HS	ADX LS+ALDO	ADX LS+ANG	ADX LS
Weight gain (3 days)	g	3.6 ± 1.7 (8)	7.5 ± 3.1 (7)	2.5 ± 2.2 (8)	4.9 ± 1.7 (8)	−29.6 ± 5.7 (8)*	−12.8 ± 2.7 (8)*
Food consumption (3 days)	g	64 ± 1.2 (8)	57 ± 5.5 (7)	54 ± 1.7 (8)	63 ± 1.0 (8)	19 ± 4.4 (8)*	38 ± 0.3 (8)*
Water intake (3 days)	ml	184 ± 28.6 (8)*	82 ± 5.5 (7)	91 ± 6.8 (8)	61 ± 5.1 (8)	23 ± 5.7 (8)	50 ± 4.2 (8)
Urine Volume (3 days)	ml	125.6 ± 28.2 (8)*	38.9 ± 3.9 (7)	49.2 ± 6.9 (8)	23.7 ± 4.1 (8)	17.1 ± 2.8 (8)	32.4 ± 1.1 (8)
Urinary Na^+ (3 days)	mmol	24.18 ± 4.21 (8)	8.76 ± 0.69 (7)	10.55 ± 1.19 (8)	0.83 ± 0.04 (7)	1.82 ± 0.36 (6)	1.63 ± 0.15 (8)
Urinary K^+ (3 days)	mmol	3.69 ± 0.38 (8)	3.4 ± 0.24 (7)	3.47 ± 0.13 (8)	2.02 ± 0.32 (8)	1.98 ± 0.14 (6)	3.06 ± 0.13 (8)
Urine osmolality at day 3	mosm/kg	626 ± 51.7 (8)	1081 ± 78.4 (7)	1142 ± 108.1 (8)	1233 ± 221.6 (8)	1055 ± 285.2 (8)	699 ± 54.1 (8)
Urine mosm (3 days)	mosm	71.13 ± 9.11 (8)	39.08 ± 2.17 (7)	41.77 ± 2.93 (8)	22.09 ± 0.97 (8)	16.36 ± 0.96 (6)	21.16 ± 0.63 (8)
Na^+ plasma at day 3	mM	134.8 ± 1.0 (5)	140.9 ± 2.5 (8)	127.5 ± 1.4 (5)	141.3 ± 4.6 (6)	138.2 ± 1.9 (8)	131.5 ± 2.4 (5)
K^+ plasma at day 3	mM	2.95 ± 0.26 (5)*	5.95 ± 0.28 (8)	5.34 ± 0.21 (5)	4.93 ± 0.37 (6)	7.27 ± 0.50 (8)*	7.38 ± 0.37 (5)*
Cl^- plasma at day 3	mM	90.3 ± 1.7 (5)	92.5 ± 2.7 (8)	93.3 ± 1.7 (5)	99.7 ± 4.6 (6)	81.9 ± 1.5 (8)	87.46 ± 3.9 (5)
Aldosterone plasma	nM	13.6 ± 4.8 (6)*	0.015 ± 0.008 (5)	0.006 ± 0.001 (7)	12.4 ± 1.5 (6)*	0.006 ± 0.001 (7)	0.020 ± 0.006 (6)
Angiotensin II plasma	pg/ml	55 ± 5.6 (5)	104 ± 23 (5)*	65 ± 5 (5)	56 ± 7.5 (5)	116 ± 17.2 (5)*	125.7 ± 17.8 (8)*

Protocol 2 involves adrenalectomized rats with hormonal replacement. Variables with the expression "3 days" include the results obtained by summing the results of the three last days before sacrifice; the expression "at day 3" refers to variables measured during the third day in the metabolic cage. Values are means ± SEM (in parentheses, the number of animals). *$P < 0.05$.

transition from an HS diet to an LS diet, there is an ≈ 10-fold decrease in crypt dextran permeability (Fig. 1*C* and Table 4). This decrease in permeability is prevented by pharmacological treatments which either prevent aldosterone synthesis (captopril or losartan) or inhibit the effect of aldosterone on the mineralocorticoid receptor (spironolactone) (Table 4). Following ADX, no decrease in dextran permeability is observed with LS diet (Table 5). However, when ADX rats, in both LS and HS conditions, are perfused with ALDO, crypt permeability to dextran is decreased ($P < 0.01$). Results from ADX rats perfused with ANG II, also show that ANG II on its own does not induce any decrease in crypt wall permeability to dextran. On the contrary, in both HS and LS conditions, the permeability to dextran increases ($P < 0.05$).

Effect of HS and LS Diet and ALDO or ANG II Supplementation post ADX on Pericryptal Na^+

Within three days of changing from HS to LS diet there is an effect on Na^+ transport in rat distal colon, evident from the raised sodium accumulation in the pericryptal spaces (Table 4). Na^+ accumulates to a higher concentration in the pericryptal sheaths of rats with a low Na^+ intake (315 ± 20 mM; $n = 5$) than in those with high Na^+ intake (150 ± 10 mM; $n = 4$). Treatment with captopril, losartan, or spironolactone prevents the increase of Na^+ transport induced by LS diet and the increase of Na^+ accumulation in the pericryptal sheath. Projection images in the Z-plane obtained using ImageJ software show that the region of high pericryptal Na^+ starts at the crypt opening and rapidly diminishes towards isotonicity at depths below 40 μm (Figure 1*A*). This correlates with the decrease in crypt luminal [Na^+] with depth. Below a crypt luminal depth of 40–50 μm, as a result of absorption from the proximal parts of the crypt, the luminal fluid is Na^+ depleted. This retards further Na^+ absorption via the colonocytes to the pericryptal sheath. With HS diet, the pericryptal Na^+ is nearly isotonic over the entire length of the crypt and no substantial decrease in luminal [Na^+] occurs. These findings with rat colon in vitro are similar to those reported previously with mouse colon in vivo (Thiagarajah et al., 2001a).

In ADX rats, in both HS and LS conditions, ALDO perfusion results in Na^+ accumulation within the pericryptal space to ≈ 330 mM. In this condition, no significant difference is observed between the pericryptal Na^+ accumulated between HS and LS conditions. When ANG II is perfused, there is no increase in pericryptal Na^+ accumulation above that in ADX rats without any supplement (Table 5).

Table 3. Electrical parameters

	PD (mV)		I_{sc} (μA/cm^2)		*TER* (Ohm • cm^2)
	basal	+amil	basal	+amil	basal
HS	1.23 ± 0.35 (4)	0.80 ± 0.15 (4)	22.2 ± 7.7 (4)	16.0 ± 7.1 (4)	52.2 ± 3.9 (3)
LS 3D	4.04 ± 2.10 (6)*	1.85 ± 0.5 (6)†	65.6 ± 10.1 (4)*	12.2 ± 5.1 (4)†	73.9 ± 4.5 (5)*
ADX HS+ALDO	4.93 ± 1.84 (4)*	0.87 ± 0.24 (4)†	98.3 ± 18.5 (5)*	13.6 ± 4.7 (4)†	62.2 ± 1.2 (7)*
ADX HS	1.65 ± 0.20 (3)	1.56 ± 0.26 (3)	38.1 ± 10.3 (3)	42.6 ± 8.2 (3)	37.6 ± 1.3 (6)
ADX LS+ALDO	4.73 ± 0.81 (5)*	0.78 ± 0.33 (5)†	99.1 ± 26.2 (4)*	15.4 ± 7.5 (4)$^\#$	55.2 ± 3.5 (10)*
ADX LS	1.73 ± 0.82 (4)	0.89 ± 0.35 (4)	53.6 ± 21.5 (4)	38.4 ± 8.4 (4)	31.4 ± 3.1 (7)

Electrical parameters obtained in distal colon tissue from HS, rats switched to LS diet for 3 days (LS 3D), adrenalectomized rats (ADX HS, ADX LS) and supplemented with ALDO (ADX HS+ALDO, ADX LS+ALDO). Values are means ± SEM (number of animals). *$P < 0.01$ marks ALDO effect; $^\dagger P < 0.01$ marks amiloride effect.

Effect of HS and LS Diet and ALDO or ANG II Supplementation post ADX on Na^+ Transport in Rat Distal Colon

LS diet increases expression of ENaC, as shown in Table 4 (and Fig. 1*B*). The density of ENaC channel γ subunit staining with immunohistochemical methods was selected as an index of comparison between treatments, as it is strongly induced by either aldosterone or a low sodium diet (Asher et al., 1996). Treatment with captopril, losartan and spironolactone inhibits the diet-induced increase of Na^+ transport (Table 4). ENaC is often difficult to localize to the apical membranes using immunohistochemical methods (Due et al., 1994). This may be due to a large reserve present within cytosolic vesicles. What is evident here is that LS diet increases the overall expression of ENaC, as has been previously observed (Garty & Benos, 1988). In ADX rats without ALDO supplementation, there is very low ENaC expression in both HS and LS conditions, with or without ANG II supplementation (Table 5). The Table also shows that when ADX rats are perfused with ALDO, in both HS and LS conditions, ENaC expression within the colonocytes is increased ($P < 0.01$, $n = 3$).

Discussion

In this paper, functional effects of HS and LS diets and hormone replacement after ADX on distal colonic function are examined. These include Na^+ accumulation in the pericryptal space, dextran permeability across the crypt wall, the electrical variables, *PD*, I_{sc} and *TER* ± amiloride (0.1 mM) and expression of ENaC in colonocytes.

Na^+ accumulation in the pericryptal sheath in vitro depends on Na^+,K^+-ATPase activity at the crypt colonocytes' basolateral membranes, ENaC activity in the crypt colonocytes apical membranes, the rates of Na^+ leakage between the pericryptal space to the crypt lumen via the paracellular and possibly transcellular routes and from the pericryptal space across the pericryptal sheath into the interstitial space. The Na^+,K^+-ATPase activity and apical membrane ENaC expression are known to be regulated by aldosterone (Barlet-Bas et al., 1988; Asher et al., 1996). The amiloride-sensitive I_{sc} mainly reflects Na^+,K^+-ATPase activity, however, it is also a function of the ion selectivity and permeability properties of the paracellular and transcellular pathways, particularly claudin IV (Colegio et al., 2003). ENaC expression is predominantly a genomic response to aldosterone. It can also be post-translationally activated by serine proteases, e.g., prostasin (Narikiyo et al., 2002). This activation may not be entirely controlled by aldosterone (Fukushima et al., 2004). Dextran permeability between the crypt lumen and the pericryptal space is principally a function of the paracellular permeability of the crypt luminal epithelia but may also reflect the permeability of the pericryptal sheath (Thiagarajah et al., 2001a and b, 2002). Thus, by observing all the variables described here, we obtain a broad spectrum of the interrelated factors controlling the transport and permeability properties of the crypt wall. The results are in agreement with the accepted view that an LS diet leads to increased aldosterone secretion, which leads in turn to increased ENaC and Na^+,K^+-ATPase expression in the mucosal border and basolateral borders of distal colon and distal nephron and, hence, to increased Na^+ transport, demonstrated here by the aldosterone-dependent amiloride-sensitive increase in I_{sc} and *PD* and by increased Na^+ accumulation in the pericryptal sheath.

The new findings are that there is an aldosterone-sensitive decrease in crypt wall permeability to dextran which correlates with the aldosterone-dependent increase in *TER*. These changes relate to the increased Na^+ accumulation in the pericryptal space as Na^+ accumulates in part because its leakage across the crypt wall is diminished.

The effects of LS cannot be unambiguously assigned to ALDO, since LS also induces an increase in

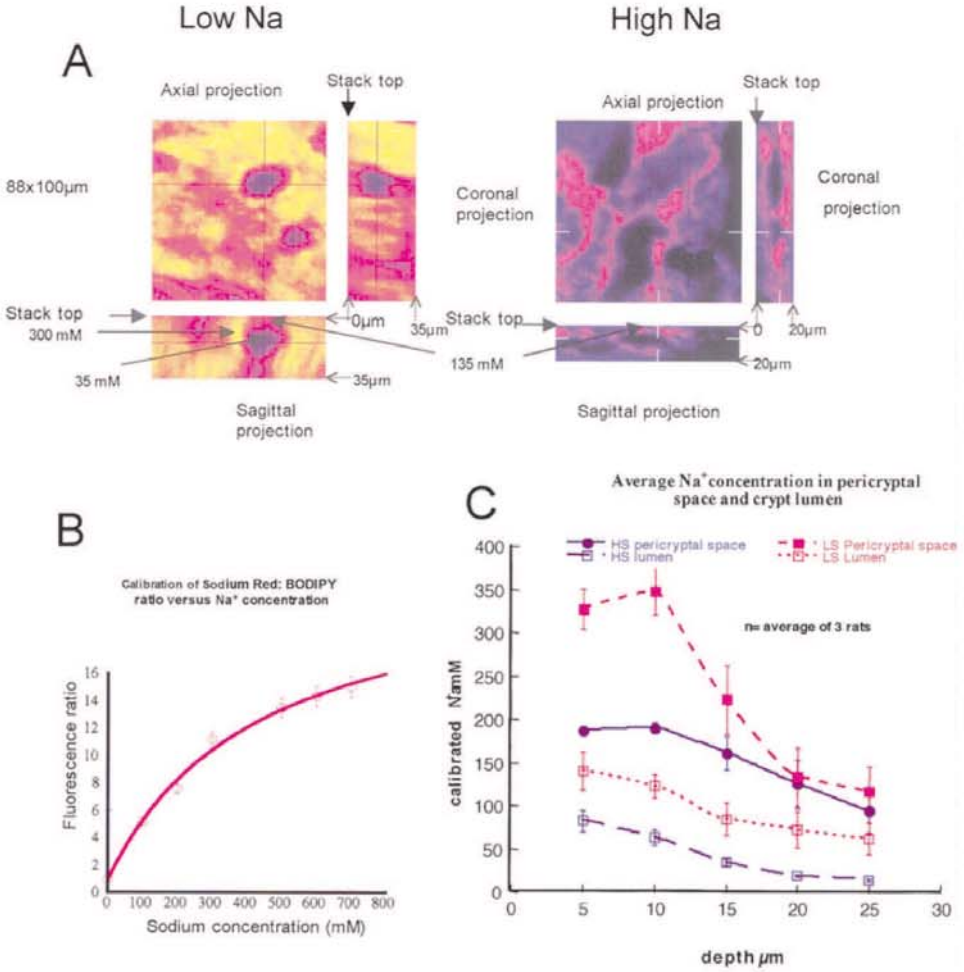

Fig. 1. Projection of stacks of confocal images of sodium red images contrasting the difference between HS and LS diet. (*A*) The projection images were obtained from stacks of ratio images taken at 0.5 µm increments in depth of colonic mucosa from HS and LS rats. These were transformed to projection images with image software (*see* Methods). The crosslines show the corresponding positions in the *x*, *y* and *z* planes in axial, coronal and sagittal sections. Thus, the sagittal projection shows the image from top at 0 µm to bottom at 35 µm depth in the stack. The color intensity varies from black to white, through red and yellow, and represents concentrations of Na^+. The Na^+ concentration in the space surrounding the crypt lumens in LS is much higher than within the lumen. The extent of these changes in Na^+ concentration with depth is shown in 1(*C*). (*B*) The pericryptal Na^+ calibrated from the ratios obtained at different Na^+ concentrations with sodium red and BODIPY-fl (*see* Methods). (*C*) The pericryptal Na^+ is on average 270–280 mM in LS rats ($n = 3$ rats) and the luminal Na^+ decreases with depth down the crypt lumen. These findings are similar to those reported by Thiagarajah et al. (2001a) for murine colon in vivo.

Table 4. Pericryptal Na^+, FITC dextran permeability and ENaC expression in Protocol 1

Protocol 1	HS	LS 3D	LS 3D CAP	LS 3D LOS	LS 3D SPI
Pericryptal Na^+ (mM)	115 ± 10 (3)	290 ± 35 (3)*	136 ± 25 (3)#	116 ± 12 (3)#	167 ± 19 (3)#
Dextran permeability (min^{-1})	0.023 ± 0001 (3)	0.002 ± 0.002 (3)*	0.019 ± 0.004 (3)#	0.029 ± 0.006 (3)#	0.025 ± 0.004 (3)#
ENaC expression (relative amount)	0.31 ± 0.05 (3)	1.01 ± 0.09 (3)*	0.38 ± 0.01 (3)*	0.14 ± 0.10 (3)#	0.45 ± 0.02 (3)#

All experiments were carried out in the distal colon segment from rats fed HS or LS diets and rats treated with captopril (CAP), losartan (LOS) and spironolactone (SPI). Values are means ± SEM. (number of animals). *$P < 0.001$ HS *vs.* LS; #$P < 0.001$ LS *vs.* pharmacological effect.

ANG II, which has been implicated in myofibroblast trophic changes in a number of tissues (Weber, 1997). For this reason, a study of the effects of ANG II and ALDO replacement following ADX in both HS and LS conditions was made to determine if dextran permeability is related to angiotensin II levels.

From the results here, it is evident that angiotensin II alone has no significant effect on Na^+

Table 5. Pericryptal Na^+, FITC dextran permeability and ENaC expression in Protocol 2

Protocol 2	ADX HS+ALDO	ADX HS+ANG	ADX HS	ADX LS+ALDO	ADX LS+ANG	ADX LS
Pericryptal Na^+ (mM)	324 ± 26 (4)*	178 ± 28 (5)	249 ± 19 (5)	331 ± 12 (4)*	172 ± 11 (5)	217 ± 13 (4)
Dextran permeability (min^{-1})	0.005 ± 0.002 (5)*	0.118 ± 0.002 (4)#	0.026 ± 0.004 (5)	0.005 ± 0.002 (4)*	0.054 ± 0.008 (4)#	0.026 ± 0.003 (4)
ENaC expression (relative amount)	0.70 ± 0.090 (3)*	0.100 ± 0.060 (4)	0.03 ± 0.1 (3)	1 ± 0.2 (3)*	0.25 ± 0.07 (4)	0.170 ± 0.090 (4)

All experiments were carried out in the distal colon segment from ADX rats and supplemented with aldosterone, angiotensin II or saline. Values are means ± SEM (number of animals). *$P < 0.01$ marks ALDO effects; #$P < 0.05$ marks Ang II effects.

transport across the crypt wall and does not reverse the HS-induced increase in crypt wall permeability to dextran. In fact, we found that dextran permeability is raised in ADX animals perfused with ANG II.

There are reports that adrenomedullin, blockade of the angiotensin II receptor I or raised intracellular cAMP can all reverse the angiotensin II-induced increases in fibrosis (Klahr & Morrissey, 1997; Swaney et al., 2005; Tsuruda et al., 2005). It is possible that ANG II without ALDO leads to breakdown of the extracellular matrix, possibly by adrenomedullin activation of matrix metalloproteinases, by as shown by Tsuruda et al. (2004). This could explain both the angiotensin II-dependent increase in dextran permeability reported here and the angiotensin II-dependent decrease in colonic transepithelial potential difference found previously (De los Rios et al., 1980).

These findings coupled with the aldosterone-dependent decrease in dextran permeability indicate that aldosterone acts not only on Na^+ transport via ENaC, Na^+, K^+-ATPase and membrane K^+ channels, but also on the less well characterized paracellular pathway. It has recently been reported that dexamethasone increases junctional proteins like claudin IV in confluent sheets of H441 lung adenocarcinoma cells prior to appearance of amiloride blockable accumulation in Na^+ domes (Shlyonsky et al., 2005). This finding is very similar to the situation observed here and reported more extensively in the companion paper (Cristià et al., 2005).

The overall conclusion is that aldosterone or mineralocorticoids, not only induce proteins which control transcellular Na^+ transport but also induce the junctional proteins which are necessary to maintain vectorial transport across epithelia and without which neither net fluid nor electrolyte flow can exist. In the descending colon, this amplification of the conventional process of transcellular water and electrolyte movement by the presence of a very impermeant paracellular route and a pericryptal sheath, are unique requirements to generate the suction tension required for fecal dehydration.

This work was supported by projects BFI2003-05124 (Ministerio de Ciencia y Tecnología, Spain) and 2001SGR0142 (Generalitat de Catalunya, Spain) and the Wellcome Trust, UK. We are grateful to Dr. Carme Villà for plasma ion determinations and the support of the Confocal Service and the ICP-OES Service, Serveis Científicotècnics, Universitat de Barcelona. E.C. was recipient of a grant from MEC (Spain).

References

Abramoff, M.D., Magelhaes, P.J., Ram, S.J. 2004. Image Processing with ImageJ. *Biophotonics Int.* **11**:36–42

Asher, C., Wald, H., Rossier, B.C., Garty, H. 1996. Aldosterone-induced increase in the abundance of Na^+ channel subunits. *Am. J. Physiol.* **271**:C605–C611

Barlet-Bas, C., Khadouri, C., Marsy Doucet, S. A. 1988. Sodium-independent in vitro induction of Na^+ K^+-ATPase by aldosterone in renal target cells: permissive effect of triiodothyronine. *Proc. Natl. Acad. Sci. USA* **85:**1707–1711

Campbell, D.J., Habener, J.F. 1986. Angiotensinogen gene is expressed and differentially regulated in multiple tissues of the rat. *J. Clin. Invest.* **78:**31–39

Campbell, S.E., Janicki, J.S., Weber, K.T. 1995. Temporal differences in fibroblast proliferation and phenotype expression in response to chronic administration of angiotensin II or aldosterone. *J. Mol. Cell. Cardiol.* **27:**1545–1560

Colegio, O.R., Van Itallie, C., Rahner, C., Anderson, J.M. 2003. Claudin extracellular domains determine paracellular charge selectivity and resistance but not tight junction fibril architecture. *Am. J. Physiol.* **284:**C1346–C1354

Cristià E., Afzal I., Pérez-Bosque A., Amat C., Moretó M., Naftalin R.J. 2005. Pericryptal colon fibrosis induced by low sodium diets is mediated by aldosterone. *J. Membrane Biol.* **206:**53–59

De los Rios, A.D., Labajos, M., Manteca, A., Morell, M., Souviron, A. 1980. Stimulatory action of angiotensin II on water and electrolyte transport by the proximal colon of the rat. *J. Endocrinol.* **86:**35–43

Dolman, D., Edmonds, C.J., Salas-Coll, C. 1978. Effect of aldosterone on lithium permeability of rat colon mucosa. *Experientia* **34:**1174–1175

Duc, C., Farman, N., Canessa, C., Bonvalet, J., Rossier, B.C. 1994. Cell-specific expression of epithelial sodium channel α,β, and γ subunits in aldosterone-responsive epithelia from the rat: localization by in situ hybridization and immunocytochemistry. *J. Cell Biol.* **127:**1907–1921

Fardella, C.E., Mosso, L. 2002. Primary aldosteronism. *Clin. Lab.* **48:**181–190

Fromm, M., Hegel, U. 1978. Segmental heterogeneity of epithelial transport in rat large intestine. *Pfluegers Arch.* **378:**71–78

Fukushima, K., Naito, H., Funayama, Y., Yonezawa, H., Haneda, S., Shibata, C., Sasaki, I. 2004. In vivo induction of prostasin mRNA in colonic epithelial cells by dietary sodium depletion and aldosterone infusion in rats. *J. Gastroenterol.* **39:**940–947

Funder, J.W., Pearce, P.T., Smith, R., Smith, A.I. 1988. Mineralcorticoid action: target tissue specificity is enzyme, not receptor, mediated. *Science* **242:**583–585

Garty, H., Benos, D.J. 1988. Characteristics and regulatory mechanisms of the amiloride-blockable Na^+ channel. *Physiol. Rev.* **68:**309–373

Hirasawa, K., Sato, Y., Hosoda, Y., Yamamoto, T., Hanai, H. 2002. Immunohistochemical localization of angiotensin II receptor and local renin-angiotensin system in human colonic mucosa. *J. Histochem. Cytochem.* **50:**275–282

Horster, M., Fabritius, J., Buttner, M., Maul, R., Weekwerth, P. 1994. Colonic-crypt-derived epithelia express induced ion transport differentiation in monolayer cultures on permeable matrix substrata. *Pfluegers Arch* **426:**110–120

Jayaraman, S., Song, Y., Vetrivel, L., Shankar, L., Verkman, A.S. 2001. Non-invasive fluorescence measurement of salt concentration in the airway surface liquid. *J. Clin. Invest.* **107:**317–324

Klahr, S., Morrissey, J.J. 1997. Comparative study of ACE inhibitors and angiotensin II receptor antagonists in interstitial scarring. *Kidney Int. Suppl.* **63:**S111–S114

Molteni, A., Moulder, J.E., Cohen, E.F. 2000. Control of radiation-induced pneumopathy and lung fibrosis by angiotensin-converting enzyme inhibitors and an angiotensin II type 1 receptor blocker. *Int. J. Radial Biol.* **76:**523–532

Naftalin, R.J. 2004. Alterations in colonic barrier function caused by a low sodium diet or ionizing radiation. *J. Envir. Path. Toxicol. Oncol.* **23:**79–97

Naftalin, R.J. Pedley, K.C. 1999. Regional crypt function in rat large intestine in relation to fluid absorption and growth of the pericryptal sheath. *J. Physiol.* **514:**211–227

Naftalin, R.J., Zammit, P.S., Pedley, K.C. 1999. Regional differences in rat large intestinal crypt function in relation to dehydrating capacity in vivo. *J. Physiol.* **514:**201–210

Narikiyo, T., Kitamura, K., Adachi, M., Miyoshi, T., Iwashita, K., Shiraishi, N., Nonoguchi, H., Chen, L., Chai, K.X., Chao, J., Tomita, K. 2002. Regulation of prostasin by aldosterone in the kidney. *J. Clin. Invest.* **109:**401–408

Paul, M., Wagner, J., Dzau, V.J. 1993. Gene expression of the renin-angiotensin system in human tissue. Quantitative analysis by the polymerase chain reaction. *J. Clin. Invest.* **91:**2058–2064

Peart, W.S. 1969. The renin-angiotensin system: a history and review of the renin-angiotensin system. *Proc. R. Soc. Lond. B.* **173:**317–325

Rasband, W.S. 1997–2005. Image J. U. S. National Institutes of Health, Bethesda, Maryland, USA, http://rsb.info.nih.gov/ij/

Schulzke, J.D., Fromm, M., Hegel, U. 1986. Epithelial and subepithelial resistance of rat large intestine: segmental differences, effect of stripping, time course, and action of aldosterone. *Pfluegers Arch.* **407:**632–637

Shlyonsky, V., Goolaerts, A., Van Beneden, R., Sariban-Sohraby, S. 2005. Differentiation of epithelial Na^+ channel function. *J. Biol. Chem.* **280:**24181–24187

Stanton, B., Giebisch, G., Klein-Robbenhaar, G., DeFronzo, R., Giebisch Wade, G.J. 1985. Effects of adrenalectomy and chronic adrenal corticosteroid replacement on potassium transport in rat kidney. *J. Clin Invest.* **75:**1317–1326

Swaney, J.S., Roth, D.M., Olson, E.R., Naugle, J.E., Meszaros, J.G., Insel, P.A. 2005. Inhibition of cardiac myofibroblast formation and collagen synthesis by activation and overexpression of adenylyl cyclase. *Proc. Natl. Acad. Sci., USA* **102:**437–442

Thiagarajah, J.R., Griffiths, N.M., Pedley, K.C., Naftalin, R.J. 2002. Evidence for modulation of pericryptal sheath myofibroblasts in rat descending colon by transforming growth factor β and angiotensin II. *Gastroenterology.* **2:**4–15

Thiagarajah, J.R., Jayaraman, S., Naftalin, R.J., Verkman, A.S. 2001a. In vivo fluorescence measurement of Na^+ concentration in the pericryptal space of mouse descending colon. *Am. J. Physiol.* **281:**C1898–C1903

Thiagarajah, J.R., Pedley, K.C., Naftalin, R.J. 2001b. Evidence of amiloride-sensitive fluid absorption in rat descending colonic crypts from fluorescence recovery of FITC-labeled dextran after photobleaching. *J. Physiol.* **536:**541–553

Tsuruda, T., Kato, J., Cao, Y.N., Hatakeyama, K., Masuyama, H., Imamura, T., Kitamura, K., Asada, Y., Eto, T. 2004. Adrenomedullin induces matrix metalloproteinase-2 activity in rat aortic adventitial fibroblasts. *Biochem. Biophys. Res. Commun.* **325:**80–84

Tsuruda, T., Kato, J., Hatakeyama, K., Masuyama, H., Cao, Y.N., Imamura, T., Kitamura, K., Asada, Y., Eto, T. 2005. Antifibrotic effect of adrenomedullin on coronary adventitia in angiotensin II-induced hypertensive rats. *Cardiovasc. Res.* **65:**921–929

Weber, K.T. 1997. Fibrosis, a common pathway to organ failure: angiotensin II and tissue repair. *Semin. Nephrol.* **17:**467–491

02.

PAPER DE L'ALDOSTERONA I DE L'ANGIOTENSINA II EN LA FIBROSI PERICRIPTAL

PERICRYPTAL MYOFIBROBLAST GROWTH IN RAT DESCENDING COLON INDUCED BY LOW-SODIUM DIETS IS MEDIATED BY ALDOSTERONE AND NOT BY ANGIOTENSIN II

E. Cristià, I. Afzal, A. Pérez-Bosque, C. Amat, R.J. Naftalin, M. Moretó

Journal of Membrane Biology 206: 53-59, 2005

Els resultats del present article s'han presentat en les següents comunicacions:

The results of the present paper have been presented in the following communications:

Cristià E, Afzal I, Pérez-Bosque A, Amat C, Moretó M, Naftalin RJ
Role of aldosterone and angiotensin II in rat colon functions during the transition from high sodium to low sodium diet

Presentat com a pòster en el congrés:

XXXIII Congreso de la Sociedad Española de Ciencias Fisiológicas (SECF). Sevilla, 10-13 Febrer 2005

Publicat a J Physiol Biochem 61:189, 2005
Premi a un dels millors pòsters del congrés.

Presented as a poster in the meeting:

XXXIII Congreso de la Sociedad Española de Ciencias Fisiológicas (SECF). Sevilla, 10-13 Feb 2005

Published in J Physiol Biochem 61:189, 2005
Awarded as one of the best poster in the congress.

Naftalin RJ, Cristià E, Afzal I, Pérez-Bosque A, Amat C, Moretó M
Role of aldosterone and angiotensin II in the trophic response of rat colon fed diets with high and low sodium content

Presentat com a pòster en el congrés:

XXXV Internacional Congress of Physiological Sciences (IUPS)
San Diego, EEUU, 31 Març-4 Abril 2005

Publicat a FASEB J 19:A750, 2005

Presented as a poster in the meeting:

XXXV Internacional Congress of Physiological Sciences (IUPS)
San Diego, EEUU, 31 March-4 April 2005

Published in FASEB J 19:A750, 2005

RESUM ARTICLE 2

Introducció: En el còlon distal de rata s'ha descrit un creixement miofibroblàstic a la zona que envolta les criptes, o zona pericriptal, que intervé en la funció absortiva del còlon. En altres teixits com el cor o el ronyó es donen estats semblant de fibrosi en situacions on està activat el RAAS, i s'hi ha descrit la implicació tant de l'angiotensina II com de l'aldosterona. En el cas del còlon, l'acció profibròtica concreta de cada una de les hormones no està definida.

Objectiu: Determinar els canvis en la fibrosi del còlon distal que es produeixen en la transició d'una dieta amb alt contingut en dosi (HS) a tres dies d'una dieta amb baix contingut en sodi (LS). Determinar el paper de l'aldosterona i l'angiotensina II per separat en la inducció d'aquest estat de fibrosi.

Material i Mètodes: Rates mascles Sprague-Dawley de 250 g de pes aproximat reben una dieta HS durant 4 dies, després dels quals, a la meitat dels animals se'ls canvia la dieta a LS. A rates d'ambdues dietes se'ls ha realitzat una adrenalectomia i se'ls ha administrat aldosterona, angiotensina II o vehicle mitjançant bombes osmòtiques per via subcutània. L'expressió de receptors de membrana, proteïnes miofibroblàstiques i de la matriu extracel.lular s'ha determinat mitjançant la tècnica d'imunohistoquímica i el posterior processament d'imatges mitjançant microscopia confocal.

Resultats: La transició d'una dieta HS a una dieta LS dóna lloc en el còlon distal a l'augment de l'expressió de molècules d'adhesió, l'E- i OB-caderina, de receptors de membrana, el receptor l'AT1 i el TGFβr1, de les unions estretes, la claudina 4, a més d'un augment en la densitat de l'ECA. A més, hi ha una proliferació dels miofibroblasts, caracteritzada per un augment de l'α-SMA i de col·lagen IV. Aquests efectes són revertits per fàrmacs inhibidors, com són el captopril, el losartan i l'espironolactona. La suplementació d'aldosterona a rates adrenalectomitzades dóna lloc a un augment de l'expressió d'α-SMA i claudina 4 similar a la dieta LS. L'angiotensina II, sense la presència d'aldosterona, no dóna lloc a l'augment d'expressió de SMA ni de col·lagen IV.

Conclusió: En tan sols tres dies de dieta LS en el còlon distal de rata es produeix un creixement miofibroblàstic a la zona pericriptal, caracteritzat per l'augment de l'expressió de α-SMA i col·lagen IV. Aquest desenvolupament de la beina de miofibroblasts en aquesta zona intestinal és estimulat per l'aldosterona, independentment de la ingesta de sodi i de la concentració d'angiotensina II.

J. Membrane Biol. 206, 53–59 (2005)
DOI: 10.1007/s00232-005-0773-4

The Journal of
Membrane
Biology

Pericryptal Myofibroblast Growth in Rat Descending Colon Induced by Low-Sodium Diets Is Mediated by Aldosterone and not by Angiotensin II

E. Cristià[2], I. Afzal-Ahmed[1], A. Pérez-Bosque[2], C. Amat[2], R.J. Naftalin[1], M. Moretó[2]
[1]Physiology Division, King's College London, Guys Campus, London, UK
[2]Departament de Fisiologia, Facultat de Farmàcia, Universitat de Barcelona, Barcelona, Spain

Received: 26 August 2005

Abstract. Pericryptal myofibroblast growth in descending colonic crypts correlates with the activation of the renin-angiotensin-aldosterone system. Earlier work showed that during the transition from a high-Na^+ (HS) to low-Na^+ (LS) diet there are changes in the colonic crypt wall and pericryptal sheath. As LS diet increases both aldosterone and angiotensin II, the aim here was to determine their individual contributions to the trophic changes in colonic crypts. Experiments were conducted on control and adrenalectomized Sprague-Dawley rats fed an HS diet and then switched to LS diet for 3 days and supplemented with aldosterone or angiotensin II. The actions of the angiotensin-converting enzyme inhibitor captopril, the angiotensin receptor antagonist losartan and the aldosterone antagonist spironolactone on extracellular matrix proteins, claudin 4 and E-cadherin myofibroblast proteins, α-smooth muscle actin (α-SMA) and OB-cadherin (cadherin 11), angiotensin type 1 and TGFβr1 membrane receptors were determined by immunolocalization in fixed distal colonic mucosa. The LS diet or aldosterone supplementation following ADX in HS or LS increased extracellular matrix, membrane receptors and myofibroblast proteins, but angiotensin alone had no trophic effect on α-SMA. These results show that aldosterone stimulates myofibroblast growth in the distal colon independently of dietary Na^+ intake and of angiotensin levels. This stimulus could be a genomic response or secondary to stretch of the pericryptal sheath myofibroblasts accompanying enhanced rates of crypt fluid absorption.

Key words: Aldosterone — Angiotensin II — Colon — Myofibroblast — Fibrosis

Correspondence to: M. Moretó; email: mmoreto@ub.edu

Introduction

A layer of myofibroblasts containing smooth muscle actin surrounds colonic crypts (Kaye, Lane & Pascal, 1968). These cells generate collagen IV and are held together predominantly by intercellular adhesion molecules, e.g., OB-cadherin (cadherin 11) (Danjo & Gipson, 1998; Hinz et al., 2004), which forms a link with the cytoskeletal smooth muscle actin (α-SMA) (Gabbiani & Badonnel, 1976) via adherens junctions in the cell membrane (Taliana et al., 2005). This cell layer has been shown to form a permeability barrier both to NaCl and dextran and to contribute to the accumulation of NaCl within the space lying between the crypt cell basal membranes and the sheath (Naftalin, Zammit & Pedley, 1995). In conditions leading to breakdown of this layer in acute post-irradiation (β or γ) colitis, when myofibroblasts apoptose within 6–12 h, or following high-sodium (HS) diet, when there is also loss of myofibroblasts, the crypts become leaky and are unable to generate a hypertonic absorbate or dehydrate feces (Thiagarajah et al., 2000; Naftalin, 2004; Moretó et al., 2005).

Colonic epithelial cells are held together mainly by the homophilic intercellular adhesion molecule, E-cadherin, via catenins at the adherens junctions (Takeichi, 1991). Tissue growth factor β (TGFβ) promotes synthesis of E-cadherins and integrins, which attach cells to the extracellular matrix at the basement membrane. Expression of both E-cadherin and integrins depends on the cells making contact with extracellular fibronectin and laminin, which activates protein kinase C, thereby maintaining the positive feedback cycle between the extracellular signal from cell contacts and the cell metabolism which maintains these contacts (Wang & Chakrabarty, 2001). Thus, the integrity of the mucosal barrier depends on the interactions between cellular and extracellular elements termed collectively cell

adhesions and cytokine stimulation cell membrane receptors (Wang et al., 2004).

Low NaCl concentrations at the macula densa segment of the renal distal tubule activate the renin-angiotensin-aldosterone system (RAAS) by increasing renin secretion, thereby inducing angiotensin I and angiotensin II (ANG II) synthesis and stimulating aldosterone (ALDO) synthesis and release in the adrenal zona glomerulosa cells (Peart, 1969). This increases both ANG II and ALDO plasma levels. Activation of RAAS by a low-sodium (LS) diet causes increased colonic fluid and Na^+ absorption (Thiagarajah et al., 2001). These effects are partly due to upregulation of the epithelial Na^+ conductance channel (ENaC) and also to changes in the barrier function of the layered structure of myofibroblasts in the pericryptal sheath, as shown in both rat (Naftalin & Pedley, 1999) and murine (Thiagarajah, Pedley & Naftalin, 2001) descending colonic crypts. Within three days of transition from HS to LS diet, the rat colonic crypt wall becomes less permeable to dextran and a much higher Na^+ concentration accumulates in the pericryptal space (Moretó et al., 2005). Retention of a high Na^+ concentration within the pericryptal space also requires that it does not drain too quickly either into the capillary circulation in the submucosa or by reflux via the paracellular route to the crypt lumen.

In cardiac tissue, RAAS activation increases periarteriolar fibrotic tissue (Weber, Sun & Katwa, 1997). This leads to myocardial hypertrophy and subsequent heart failure. The primary cause of the increased myocardial fibrosis is invasion of the damaged tissue by macrophages and transformation of fibroblasts to myofibroblasts; these cells in turn produce cytokines, TGFβ, endothelin 1, and connective tissue growth factor that further stimulate myofibroblasts to generate collagen (Campbell & Katwa, 1997). The temporo-spatial coincidence of angiotensin-converting enzyme (ACE) activity and ANG II type 1 receptors (ATr1) has been observed at sites of fibrosis (Sun, Ramires & Weber, 1997). High densities of ACE antibody-binding have been observed at repair sites one week after myocardial infarction (Falkenhahn et al., 1995; Mezzano et al., 2003). The presence and density of ATr1 and TGFβr1 receptors has been shown to be a key factor in development of fibrosis. In cardiac myofibroblasts, Campbell, Janicki & Weber (1995) and Campbell and Katwa (1997) observed that ANG II has trophic effects, increasing α-SMA expression after 2 days, and increasing collagen synthesis after 14 days of infusion. TGFβ released by myofibroblasts leads to further release of cytokines by the myofibroblasts, resulting in a positive feedback loop, which leads to overproduction of collagen by the stimulated myofibroblasts and prevention of apoptosis (Zhang & Phan, 1999)

Angiotensin-converting enzyme inhibitors do not suppress ALDO synthesis completely. Mineralocorticoid receptors (MR) have been detected in cardiac myocytes and endothelial cells (Lombèd et al., 1995) and ALDO infusion produced cardiac fibrosis that can be prevented by spironolactone (Brilla et al., 1994). This leads to cardiac remodeling and eventual failure (Soberman, Chafin & Weber, 2002). The RALES trial (Zannad et al., 2000), which evaluated the benefits of spironolactone therapy on congestive heart failure, showed that ALDO-receptor blockade decreased morbidity and mortality associated with excessive myofibroblast stimulation.

As in heart and kidney, RAAS-related events in the distal colon stimulate fibrosis by stimulating myofibroblast growth (Thiagarajah et al., 2002).

Currently the specific effect(s) of ANG II and ALDO on myofibroblast growth are unclear. Transformation of fibroblasts to myofibroblasts has been attributed both to ALDO and ANG II and more recently to synergism between low concentrations of ALDO and ANG II (Min et al., 2005).

The main purpose of this present study is to discriminate between the two possible modes of stimulation of the trophic changes in colon by the RAAS. This has been done in two steps, first by observing the effects of ANG II inhibition by ACE inhibition with captopril, or ATr1 antagonism with losartan, or with the ALDO antagonist, spironolactone. As the results from these early studies left some uncertainty about whether ALDO alone, or ALDO in combination with ANG II was responsible for the trophic effects on colon, a second series of experiments was undertaken in which adrenalectomy (ADX) with infusion of either ALDO, or ANG II post-ADX, to replace one or other missing hormones, was tested to determine the extent to which these hormones activated the trophic effects on their own. Specifically, to test whether the adaptive effects in colon following LS are due to raised ALDO or to raised ANG II and whether the effects of the two hormones are synergistic. Although the current results unequivocally show that aldosterone is the trophic agent and ANG II alone does not cause a positive trophic effect on the myofibroblast layer—it may induce a negative trophic effect—doubts remain concerning synergy between ALDO and ANG II or synergism between ALDO and other factors influencing myofibroblast development.

Materials and Methods

Experimental Animals

Studies were performed on adult male Sprague-Dawley rats (Harlan Ibérica, Barcelona, Spain) weighing 200–250 g the day of experiment. Animals were housed one per cage under 12:12-h light-dark cycle,

and food and water were available *ad libitum*. Experimental procedures were approved by the ethical committee of the Universitat de Barcelona. The following two protocols were undertaken.

Protocol 1: The effects of HS and LS Diets and Pharmacological Treatment Modifying These

Animals received an HS diet (wheat and barley and drinking water containing 150 mM NaCl). After 4 days, animals were changed to a LS diet (wheat and barley and drinking water containing 150 μM NaCl) for 3 days. When appropriate, rats received pharmacological treatment: captopril (CAP, ACE inhibitor; 65 mg/kg·day in drinking water), losartan (LOS, ATr1 receptor inhibitor; 30 mg/kg.day in drinking water) or spironolactone (SPI, ALDO antagonist; 10 mg/kg·day by oral gavage).

Protocol 2: The Effects of HS and LS Diets in Adrenalectomized Rats Followed by Selective Hormonal Replacements

Rats were adrenalectomized (ADX) via bilateral flank under isofluorane (Inibsa®, Spain) anaesthesia. The protocol performed was as described before (Moretó et al., 2005). Briefly, osmotic minipumps (model 2002, Alzet, Palo Alto, CA) were implanted subcutaneously in the upper back region following ADX procedures. Pumps were filled with D-aldosterone (Sigma) dissolved in propylene glycol or with ANG II (Sigma) dissolved in saline, to deliver 450 μg/kg/day or 288 μg/kg/day, respectively. This protocol led to chronic increases in the plasma concentrations of both hormones. Groups without hormonal replacement were implanted with pumps delivering vehicle.

After surgery the animals were kept on the HS diet for 4 days. Thereafter, half of the animals were changed to LS diet for 3 days and the other half continued with HS diet. With this protocol 6 groups with different hormone profiles are obtained: ADX HS + ALDO, ADX HS + ANG, ADX HS, ADX LS + ALDO, ADX LS + ANG and ADX LS.

Tissue Preparation

Rats from both protocols were maintained in metabolic cages for the last three days prior to sacrifice, and the daily 24-h urinary output, water intake, food consumption and body weight were measured as described (Moretó et al., 2005). The descending colon was rapidly excised and the contents removed by washing with buffer. Mucosal sheets scraped from the underlaying serosa were fixed (4% paraformaldehyde in PBS) at 4°C for 24 h. The tissue was then washed and stored in PBS at 4°C for immunocytochemistry.

Immunocytochemistry

Colonic mucosal tissues (0.5 cm^2 pieces) were placed in 1.5 mL Eppendorf tubes. Tissues were then stained according to the following protocol. The procedure was the same for all antibodies used. Tissues were permeabilized in 0.2% Triton X-100 in blocking buffer (1% BSA in PBS and glycine) for 30 min. Samples were washed three times in PBS and incubated for 90 min with primary antibody (1:100), washed 3× in PBS and then incubated for 60 min in each secondary antibody (1:100) and washed again 3× in PBS.

Antibodies

The antibodies were obtained from the following agencies: Chemicon: RDI rabbit anti-collagen Type IV, mouse anti-angiotensin converting enzyme (ACE), monoclonal and rabbit anti-ANG II Type 1 receptor; Sigma: monoclonal anti-α smooth muscle actin α-SMA clone IA4; Santa Cruz: rabbit anti-TGFβ receptor 1 (R-20), goat anti-OB cadherin (Cadherin-11). For ANG II type 1 receptor-, TGFβr1-, and collagen IV-stained tissue, biotin anti-rabbit IgG was used as the secondary antibody followed by Alexa-488 NeutrAvidin. For ACE- and anti-α SMA-staining, Texas Red goat anti-mouse IgG was used. All secondary antibodies and Alexa-488 were obtained from Molecular Probes (Eugene, OR); goat anti-cadherin-E (human/mouse/rat), from Research Diagnostics (RDI, UK).

Confocal Images

Each piece of tissue was viewed in a Leica SPII confocal microscope using a 20 × oil immersion lens (Barcelona University), or using a Nikon Diaphot inverted microscope with Nikon Fluor 20× and 60× lenses attached to a BioRad MRC 600 confocal scanhead, equipped with two detection channels and an Ar/Kr mixed-gas laser allowing excitation at 488 nm and 568 nm (King's College London). *Z*-Axis movement with 0.1 μm resolution was provided by a software-controlled stepper motor attached to the fine focus control. The tissue was viewed from the mucosal side. The focus plane was initially taken to the surface of the tissue and images were captured at 5 μm steps from 0 μm down to 40–100 μm below the surface. The chosen images represented as much as possible the general level of staining throughout the whole tissue and were captured with the same optical conditions, gain and section size. Because the intensity of the image fluorescence varies with depth and because of slight tissue folding, the exact depth of the *Z*-plane cannot be accurately quantified to better than 5–10 μm; for this reason average intensity projection images in the *Z*-plane over the planes 5–40 μm were used to give comparability between samples from different pieces of tissue. This is easily done with colonic mucosa viewed *en face* since the crypts and their surrounding spaces lie perpendicular to the surface plane over a depth of at least 100 μm.

Image Analysis

The images were analyzed using ImageJ program (http://rsb.info.nih.gov/ij/index.html). Fluorescence was quantified by dividing the field into either "crypt" or "intercryptal" areas by selecting regions of interest (ROI) within the relevant part of the image by drawing around the crypts with the freehand drawing tool. Three areas of both crypt and intercrypt were taken per image. After background subtraction, the mean and SEM of measurements from each image were calculated.

Statistics

Data were expressed as means ± SEM. Comparisons between HS and LS diet were made by ANOVA using SPSS-10.0 software (SPSS). To analyze the effects of pharmacological treatment, groups were compared with the LS group by ANOVA, followed by Scheffé's *post-hoc* test. In ADX groups, the groups with ALDO or ANG II replacement were compared with the groups without supplementation by ANOVA followed by Scheffé's *post-hoc* test. Differences were considered statistically significant when the test yielded $P < 0.05$.

Results

Characteristics of the Model

The changes in body weight, food and water intake, physiological variables relating to the urinary func-

tion, plasma ion and hormone concentrations are described in the previous paper (Moretó et al., 2005). Briefly, the groups on HS and LS diets showed the expected marked differences in urinary Na^+ excretion and ALDO and ANG II plasma concentration. In ADX animals (Protocol 2), hormonal replacement raised circulating ALDO (13.6 ± 4.8 nM in ADX HS + ALDO group, $n = 6$; 12.4 ± 1.5 nM in ADX LS + ALDO group, $n = 6$) and ANG II (104 ± 23 pg/mL in ADX HS+ANG, $n = 5$; 116 ± 17 pg/mL in ADX LS+ANG, $n = 5$). The two adrenalectomized groups without hormone infusion had no detectable levels of plasma ALDO.

Effect of HS and LS Diet on the Pericryptal Sheath

The hypothesis that ANG II regulates colonic fibrosis predicts that the receptors mediating this effect would be increased by the LS diet. After 3 days LS diet, TGFβr1 and ATr1 expression in the pericryptal region is increased by 5-fold and 38-fold respectively. These increases were prevented by captopril. However, neither losartan, nor spironolactone blocked the increases in ATr1. Since neither of the latter treatments interferes with ANG II synthesis, whereas losartan blocks ALDO synthesis and spironolactone blocks ALDO binding to the MR receptor, it may be inferred that ANG II is solely responsible for the observed increase in ATr1 (Fig. 1).

Similar effects of LS diet following HS diet on ACE density were observed. Following HS diet, there is a significant increase in expression of ACE, which is significantly reduced in LS by captopril (Figure 2).

Hormonal Effects on Paracellular Route

Myofibroblasts in the pericryptal layers are held together by OB-cadherin (Hinz et al., 2004) and colonocytes by E-cadherin (Takeichi, 1991) and both adhesion molecules are required for anchorage to underlying cytoskeletal elements. Results show that the LS diet increases by 14-fold and 2.4-fold the expression of OB-cadherin and E-cadherin, respectively, compared with the HS diet ($P < 0.05$ in all cases, Table 1). Captopril blocked the expression of OB-cadherin induced by diet, but did not prevent the expression of E-cadherin.

Claudins are junctional proteins that participate in epithelial barrier function and regulate paracellular permeability (Van Itallie, Rahner & Anderson, 2001; Matter & Balda, 2003). The expression of claudin IV was increased by an LS diet compared with the HS diet. The three pharmacological treatments prevented this effect (Fig. 1). In ADX groups, infusion of ALDO increased the expression of crypt colonocyte claudin IV independently of the sodium content of the diet ($P < 0.01$ for ALDO perfusion vs zero ALDO for both HS and LS) showing that ALDO can regulate the colonocyte tight junction structure. ALDO has recently been shown to induce an early acute effect on phosphorylation of claudin IV in cultured renal collecting duct cells (Le Moellic et al., 2005). This change is accompanied by reduced mannitol permeability.

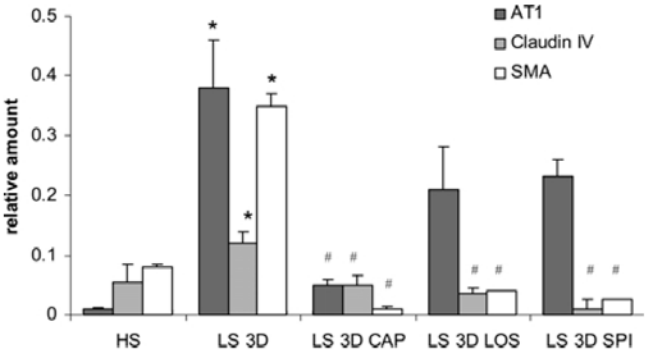

Fig. 1. Expression of ATr1, Claudin IV and α-smooth muscle actin (α-SMA) in control and pharmacologically treated groups. Values are means ± SEM ($n = 4$ animals). $^*P < 0.01$ HS *vs.* LS; $^{\#}P < 0.01$ LS *vs.* pharmacological treatment.

Effects on the Pericryptal Sheath Myofibroblasts Induced by Hormones

Once it was demonstrated in colon that expression of two receptors, TGFβr1 and ATr1, which activate fibrosis, ascribed to ANG II, was increased by the LS diet (Fig. 1), we decided to test whether ANG II had direct trophic effects on the pericryptal sheath similar to those reported in cardiac tissue (Campbell et al., 1995). Thus, expression of smooth muscle actin (α-SMA), a protein present in myofibroblasts (Gabbiani & Badonnel, 1976), and collagen IV, an exclusive myofibroblast product, was studied in the pericryptal sheaths of descending colonic crypts.

LS diet increases the amount of α-SMA in the pericryptal sheath by 4-fold (Fig. 1), while the fluorescence signal for collagen IV is increased 3-fold (Table 1). Captopril or losartan or spironolactone prevents the stimulatory effect of LS on α-SMA expression. In ADX animals, infusion of exogenous ALDO increased the amount of pericryptal α-SMA in both LS and HS conditions but to a greater extent in LS ($P < 0.01$ for both ALDO perfusion vs. control in HS and LS conditions) (Fig. 4). ANG II administration did not stimulate the expression of α-SMA in ADX rats. These results suggest that only ALDO has trophic effects on myofibroblast proliferation.

Discussion

Prolonged low Na^+ intake results in functional adaptations affecting the capacity of the distal

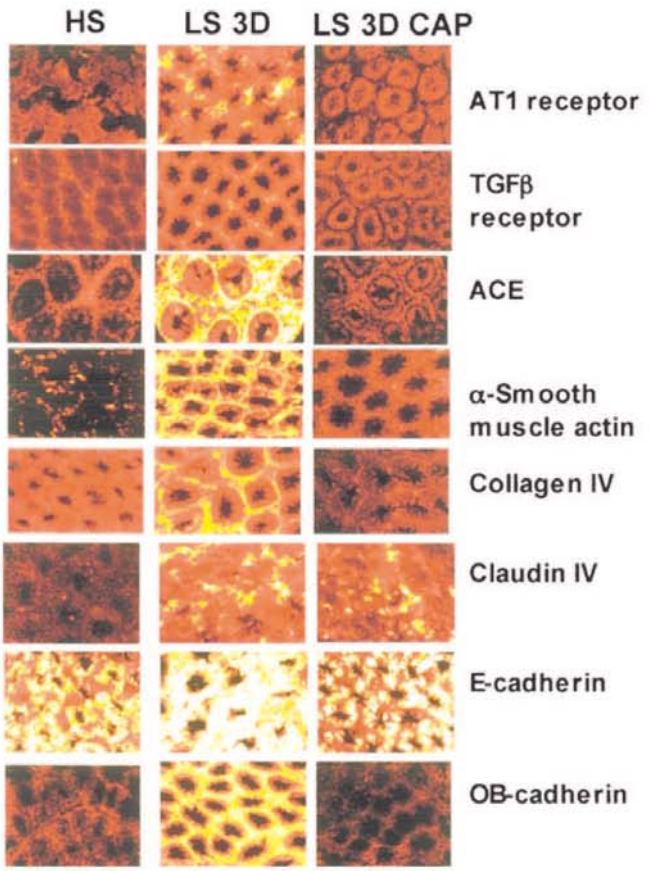

Fig. 2. Confocal images showing the LS diet ± captopril (*CAP*) effect on crypt antigen expression. All images were taken at a depth of 20 μm from the tissue surface.

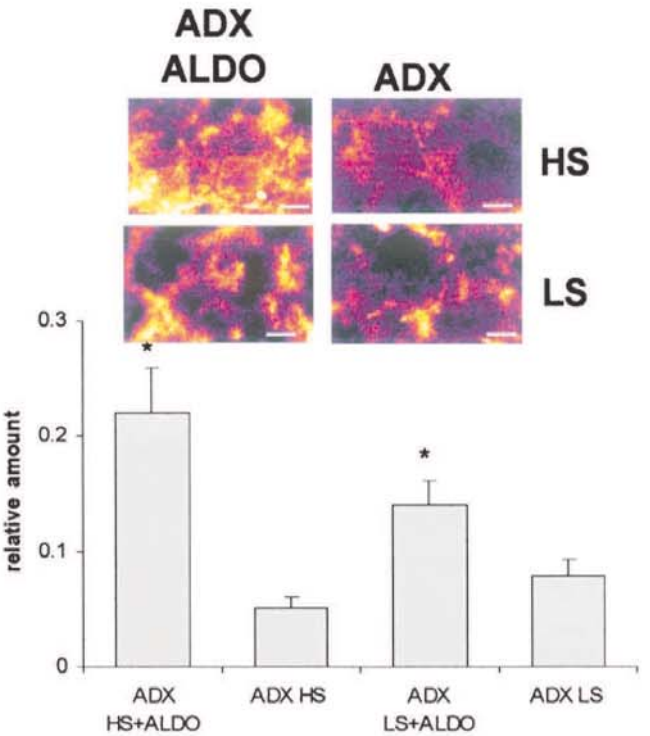

Fig. 3. Expression of Claudin IV in ADX groups supplemented with ALDO, ANG II or vehicle. Values are means ± SEM (n = 3–5 animals). Confocal images show Claudin IV-images taken at a depth of 20 μm from the tissue surface. *$P < 0.05$.

nephron and the distal colon to reabsorb Na^+; trophic effects accompany these functional changes in distal colon. Thiagarajah et al. (2002) showed that after 10 days of LS diet there was a growth stimulus of the pericryptal sheath cells surrounding the crypts of the descending colon, with increases in collagen IV deposition and OB-cadherin, smooth muscle actin, ACE and both ATr1 and TGFβr1 receptor expression. As an LS diet increases both ANG II and ALDO levels (Moretó et al., 2005), the main goal of the present study was to show whether ALDO or ANG II alone or in combination is required to generate the full trophic response of colonic crypts. The present study shows that these changes are detectable within 3 days of transition from HS to LS diet. Additionally, claudin IV, a protein that regulates tight junction permeability (Figs. 2 and 3) and E-cadherin (Fig. 2), an intercellular adhesion molecule, were increased by the LS diet. These results show that the growth of the pericryptal sheath during LS adaptation is concurrent with increased transepithelial Na^+ transport (Moretó et al., 2005), and confirm that colonic absorptive function depends both on crypt luminal cells and on myofibroblasts cells (Naftalin & Pedley, 1999).

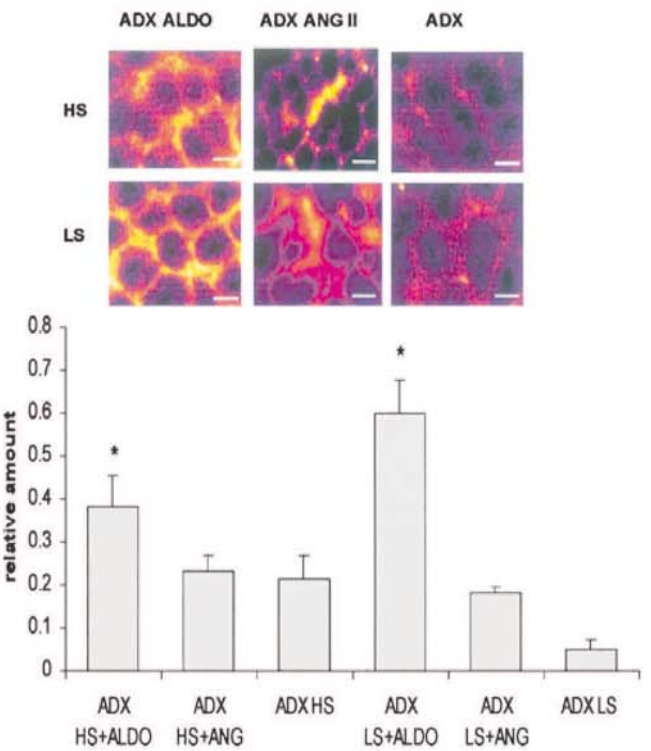

Fig. 4. Expression of α-smooth muscle actin (α-SMA) in ADX groups supplemented with ALDO, ANG II or vehicle. Values are means ± SEM (n = 5 animals). Confocal images show SMA images taken at a depth of 20 μm from the tissue surface. *$P < 0.05$.

Table 1. TGFβr1, OB-cadherin, E-cadherin, ACE and collagen IV expression using Protocol 1

	HS	LS 3D	LS 3D CAP
TGFβ receptor	0.05 ± 0.01 (5)	0.23 ± 0.008 (5)*	0.08 ± 0.002 (5)$^{\#}$
OB-cadherin	0.30 ± 0.03 (5)	4.31 ± 1.01 (5)*	0.23 ± 0.01 (5)$^{\#}$
E-cadherin	0.05 ± 0.02 (5)	0.12 ± 0.01 (5)*	0.12 ± 0.04 (5)
ACE	1.45 ± 0.20 (5)	2.08 ± 0.17 (5)*	1.51 ± 0.12 (5)$^{\#}$
Collagen IV	0.01 ± 0.0005 (5)	0.03 ± 0.0010 (5)*	0.01 ± 0.0005 (5)$^{\#}$

All experiments were carried out in the distal colon segment from rats fed HS or LS diets and rats treated with captopril (CAP). Values are relative amounts, expressed as means ± SEM; (number of animals in parentheses). *$P < 0.001$ HS *vs.* LS; $^{\#}P < 0.001$ LS *vs.* pharmacological effect.

The ACE inhibitor, captopril, the ATr1 receptor antagonist, losartan, and the ALDO antagonist, spironolactone, were investigated to determine which specific regulatory agent is involved in the trophic changes in descending colon (Fig. 1). Unfortunately for present purposes, inhibition of ANG II synthesis also indirectly decreases ALDO synthesis (Moretó et al., 2005), so the inhibition of the effect of LS with captopril or losartan could be due to loss of stimulation from either ANG II or ALDO.

The large reductions of the expression of myofibroblast smooth muscle actin and the intercellular junctional proteins, claudin IV and E- and OB-cadherin, seen in LS modulated by spironolactone, are unequivocal evidence for the requirement of ALDO (Table 1, Fig. 1). The results (Fig. 4) also indicate that ANG II alone has no trophic effect on crypt myofibroblasts. However, the possibility that there is a synergistic effect of ANG II and ALDO cannot be excluded by this result.

Until recently, our hypothesis was that ALDO controlled ENaC and Na^+ pump levels, whilst ANG II controlled the myofibroblastic pericryptal sheath growth. This was based on our experiments with the ACE inhibitor captopril, which slowed colonic adaptation to LS diet. However, the more recent experiments with osmotic minipumps (Moretó et al., 2005) confound these simple findings. ADX animals maintained on HS diets, where ANG II levels are low, given ALDO by continuous injection with a minipump, have a smooth muscle actin expression as high as colon adapted to LS diet (Table 1). Apparently, raised ALDO alone can stimulate myofibroblast growth. Similar findings have been reported in cardiac muscle (Funder, 2001).

Although our results in both this and the companion paper (Moretó et al., 2005) indicate that ANG II perfusion in the ADX has no positive trophic effect on the extracellular matrix. Indeed, in view of the raised dextran permeability and transepithelial tissue resistance observed in this condition, it is likely that ANG II perfusion in the absence of aldosterone inhibits collagen synthesis-possibly by ANG II-dependent activation of adrenomedullin, which in turn activates collagenases in the extracellular matrix (Mishima et al., 2003; Tsuruda et al., 1999, 2004).

It is also uncertain that the positive trophic response of myofibroblasts to ALDO treatment is entirely a genomic response. Several recent studies indicate that as well as ALDO-induced growth of myofibroblasts, mechanical tension stress modulates myofibroblasts' smooth muscle actin synthesis and contractile strength (Hinz et al., 2004; Taliana et al., 2005). Additionally, the rapid phosphorylation of claudin 4 in response to ALDO (Le Moellic et al., 2005) suggests that other non-genomic factors, e.g., local mechanical stress induced by fluid transport itself, could be factors in the apparent trophic effects of ALDO in mesenchymal tissue surrounding the crypts.

This work was supported by projects BFI2003-05124 (Ministerio de Ciencia y Tecnología, Spain) and 2001SGR0142 (Generalitat de Catalunya, Spain). We are grateful to Maria Balda for Claudin 4 antibody, Dr. Carme Villà for plasma ion determinations and the support of the Confocal Service and the ICP-OES Service, Serveis Cientificotecnics, Universitat de Barcelona. E.C. was recipient of a grant from MEC (Spain).

References

Brilla, C.G., Zhou, G., Matsubara, L., Weber, K.T. 1994. Collagen metabolism in cultured adult rat cardiac fibroblasts:response to angiotensin II and aldosterone. *J. Mol. Cell. Cardiol.* **26:**809–820

Campbell, S.E., Janicki, J.S., Weber, K.T. 1995. Temporal differences in fibroblast proliferation and phenotype expression in response to chronic administration of angiotensin II or aldosterone. *J. Mol. Cell. Cardiol.* **27:**1545–1560

Campbell, S.E., Katwa, L.C. 1997. Angiotensin II stimulated expression of transforming growth factor-beta1 in cardiac fibroblasts and myofibroblasts. *J. Mol. Cell. Cardiol.* **29:**1947–1958

Danjo, Y., Gipson, I.K. 1998. Actin 'purse string' filaments are anchored by E-cadherin-mediated adherens junctions at the leading edge of the epithelial wound, providing co-ordinated cell movement. *J. Cell Sci.* **111:**3323–3332

Falkenhahn, M., Franke, F., Bohle, R.M., Zhu, Y.C., Stauss, H.M., Bachmann, S., Danilov, S., Unger, T. 1995. Cellular distribution of angiotensin-converting enzyme after myocardial infarction. *Hypertension* **25:**219–226

Funder, J.W. 2001. Mineralocorticoids and cardiac fibrosis: the decade in review. *Uni. Exp. Pharmacol. Physiol.* **28:**1002–1006

Gabbiani, G., Badonnel, M.C. 1976. Contractile events during inflammation. *Agents Actions* **6:**277–280

Hinz, B., Pittet, P., Smith-Clerc, J., Chaponnier, C., Meister, J.J. 2004. Myofibroblast development is characterized by specific cell-cell adherens junctions. *Mol. Biol. Cell* **15:** 4310–4320

Kaye, G.I., Lane, N., Pascal, R.R. 1968. Colonic pericryptal fibroblast sheath: replication, migration and cytodifferentiation of a mesenchymal cell system in adult tissue. II. Fine structural aspects of normal rabbit and human colon. *Gastroenterology* **54:**852–865

Le Moellic, C., Boulkroun, S., Gonzalez-Nunez, D., Dublineau. I., Cluzeaud. F., Fay, M., Blot-Chabaud, M., Farman, N. 2005. Aldosterone And Tight Junctions: Modulation Of Claudin 4 Phosphorylation In Renal Collecting Duct Cells. Am. J. Physiol. **289:** C1513–C1521

Lombèd, M., Alfaidy, N., Eugene, E., Lesana, A., Farman, N., Bonvalet, J.P. 1995. Prerequisite for cardiac aldosterone action. *Circulation* **92:**175–182

Matter, K., Balda, M.S. 2003. Signalling to and from tight junctions. *Nat. Rev. Mol. Cell Biol.* **4:**225–236

Mezzano, S.A., Aros, C.A., Droguett, A., Burgos, M.E., Ardiles, L.G., Flores, C.A., Carpio, D., Vio, C.P., Ruiz-Ortega, M., Egido, J. 2003. Renal angiotensin II up-regulation and myofibroblast activation in human membranous nephropathy. *Kidney Int. Suppl.* **86:**39–45

Min, L.J., Mogi, M., Li, J.M., Iwanami, J., Iwai, M., Horiuchi, M. 2005. Aldosterone and Angiotensin II Synergistically Induce Mitogenic Response in Vascular Smooth Muscle Cell. *Circ. Res.* **97:** 434–442

Mishima, K., Kato, J., Kuwasako, K., Imamura, T., Kitamura, K., Eto, T. 2003. Angiotensin II modulates gene expression of adrenomedullin receptor components in rat cardiomyocytes. *Life Sci.* **73:**1629–1635

Moretó, M., Cristià, E., Pérez-Bosque, A., Afzal-Ahmed, I., Amat, C., Naftalin, R.J. 2005. *J. Membrane Biol.* **206:**43–51

Naftalin, R.J. 2004. Alterations in colonic barrier function caused by a low sodium diet or ionizing radiation. *J. Envir. Pathol. Toxicol. Oncol.* **23:**79–97

Naftalin, RJ., Pedley, K.C. 1999. Regional crypt function in rat large intestine in relation to fluid absorption and growth at the pericryptal sheath. *J. Physiol.* **514.1:**211–227

Naftalin, R.J., Zammit, P.S., Pedley, K.C. 1995. Concentration polarization of fluorescent dyes in rat descending colonic crypts: evidence of crypt fluid absorption. *J. Physiol.* **487:**479–495

Peart, W.S. 1969. The renin-angiotensin system: a history and review of the renin-angiotensin system. *Proc. R. Soc. Lond. B.* **173:**317–325

Soberman, J., Chafin, C.C., Weber, K.T. 2002. Aldosterone antagonists in congestive heart failure. *Curr. Opinion Investig. Drugs* **3:**1024–1028

Sun, Y., Ramires, F.J., Weber, K.T. 1997. Fibrosis of atria and great vessels in response to angiotensin II or aldosterone infusion. *Cardiovasc. Res.* **35:**138–147

Takeichi, M. 1991. Cadherin cell adhesion receptors as a morphogenetic regulator. *Science* **251:**1451–1455

Taliana, L., Benezra, M., Greenberg, R.S., Masur, S.K., Bernstein, A.M. 2005. ZO-1: Lamellipodial localization in a corneal fibroblast wound model. *Invest. Ophthalmol. Vis. Sci.* **46:**96–103

Thiagarajah, J.R., Gourmelon, P., Griffiths, N.M., Lebrun, F., Naftalin, R.J., Pedley, K.C. 2000. Radiation induced cytochrome c release causes loss of rat colonic fluid absorption by damage to crypts and pericryptal myofibroblasts. *Gut* **47:**675–684

Thiagarajah, J.R., Griffiths, N.M., Pedley, K.C., Naftalin, R.J. 2002. Evidence for modulation of pericryptal sheath myofibroblasts in rat descending colon by transforming growth factor and angiotensin II. *BMC Gastroenterology* **2:**4–15

Thiagarajah, J.R., Pedley, K.C., Naftalin, R.J. 2001. Evidence of amiloride-sensitive fluid absorption in rat descending colonic crypts from fluorescence recovery of FITC-labeled dextran after photobleaching. *J. Physiol.* **536:**541–553

Tsuruda, T., Kato, J., Kitamura, K., Kawamoto, M., Kuwasako, K., Imamura, T., Koiwaya, Y., Tsuji, T., Kangawa, K., Eto, T. 1999. An autocrine or a paracrine role of adrenomedullin in modulating cardiac fibroblast growth. *Cardiovasc. Res.* **43:**958–967

Tsuruda, T., Kato, J., Cao, Y.N., Hatakeyama, K., Masuyama, H., Imamura, T., Kitamura, K., Asada, Y., Eto, T. 2004. Adrenomedullin induces matrix metalloproteinase-2 activity in rat aortic adventitial fibroblasts. *Biochem. Biophys. Res. Commun.* **325:**80–84

Van Itallie, C., Rahner, C., Anderson, J.M. 2001. Regulated expression of claudin 4 permeability. *J. Clin. Invest.* **107:**1319–1327

Wang H., Chakrabarty, S. 2001. Requirement of protien kinase Calpha, extracellular matrix remodeling, and cell-matrix interaction for transforming growth factor-regulated expression of E-cadherin and catenins. *J. Cell Physiol.* 187:188–195

Wang, H., Radjendirane, V., Wary, K.K., Chakrabarty, S. 2004. Transforming growth factor beta regulates cell-cell adhesion through extracellular matrix remodeling and activation of focal adhesion kinase in human colon carcinoma Moser cells. *Oncogene* **15:**5558–5561

Weber, K.T., Sun, Y., Katwa, L.C. 1997. Myofibroblasts and local angiotensin II in rat cardiac tissue repair. *Int. J. Biochem. Cell Biol.* **29:**31–42

Zannad, F., Alla, F., Dousset, B., Perez, A., Pitt, B. 2000. Limitation of excessive extracellular matrix turnover may contribute to survival benefit of spironolactone therapy in patients with congestive heart failure: insights from the randomized aldactone evaluation study (RALES). *Circulation* **102:**2700–2706

Zhang, H.Y., Phan, S.H. 1999. Inhibition of myofibroblast apoptosis by transforming growth factor β1. *Am. J. Respir. Cell. Mol. Biol.* **21:**658–665

MANUSCRIPT

MANUSCRIT

03.

PAPER DE LA VASOPRESSINA EN LA FUNCIÓ DEL CÒLON DISTAL

VASOPRESSIN AND CRYPT COLON FUNCTION IN RATS FED DIETS WITH HIGH AND LOW SODIUM CONTENT

E. Cristià, C. Amat, R.J. Naftalin, M. Moretó

Els següents resultats es presenten en forma de manuscrit. L'escrit tal i com es presenta en aquesta tesi ha estat enviat a la revista "Journal of Physiology".

The following results are presented as a manuscript. It has been sent to the "Journal of Physiology".

Part dels estudis que es recopil·len en aquest apartat s'han realitzat al King's College London durant una estada de 4 mesos sota la direcció del Dr. Richard Naftalin (Beca d'estades breus, FPU, MEC).

Some of the results included in this section have been realized in the King's College London, during a 4 month stage with the direction of Prof. Richard Naftalin (Grant, FPU, MEC).

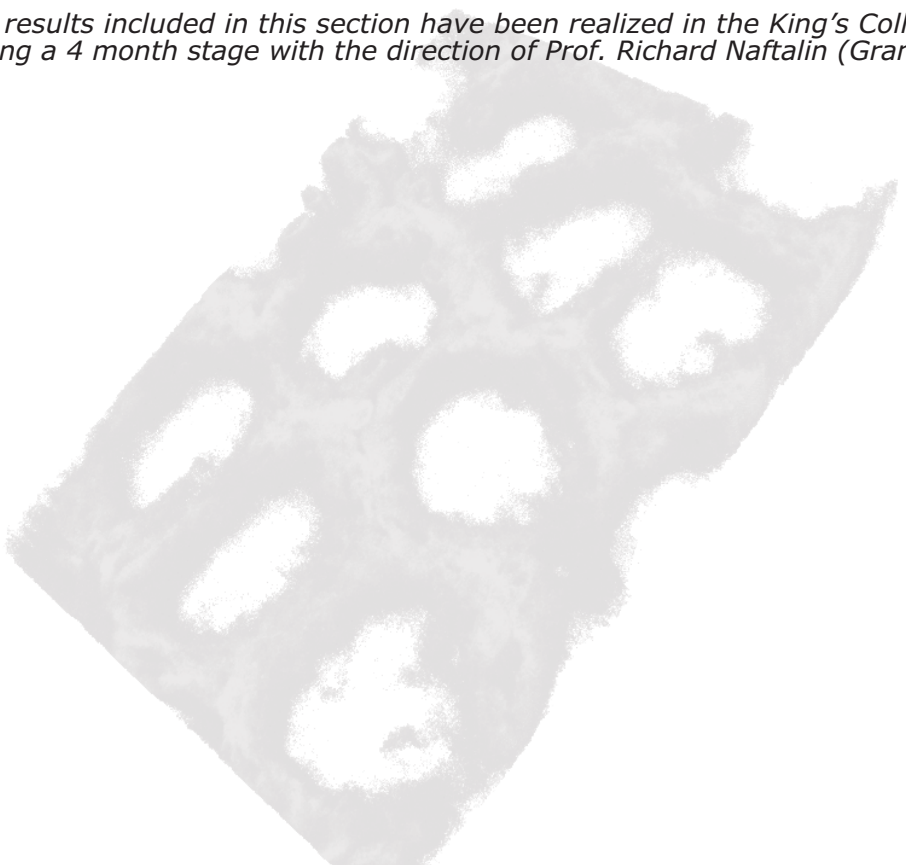

RESUM MANUSCRIT

Introducció: La vasopressina intervé en els mecanismes d'homeòstasi hídrica i electrolítica en el còlon distal, s'ha descrit que actua sinèrgicament amb l'aldosterona en diferents accions tant al ronyó com al còlon i sembla intervenir en el creixement de la matriu extracel·lular al cor i al ronyó.

Objectiu: Determinar l'acció de la deshidratació i de la vasopressina en la funció del còlon distal de rata i determinar possibles accions sinèrgiques o de col·laboració amb l'aldosterona en dietes amb alt i baix contingut en sodi. Determinar el paper de cada un dels receptors de la vasopressina en aquestes funcions.

Material i Mètodes: L'estudi s'ha realitzat amb rates mascles Sprague-Dawley de 250 g de pes aproximat alimentades amb dietes HS o LS i a les quals se'ls ha restringit l'aigua de beguda durant 24h o se'ls ha administrat vasopressina mitjançant bombes osmòtiques. Algunes rates reben antagonistes específics per cada un dels receptors de vasopressina; el *Manning Peptide* com a antagonista V_1 i el Tolvaptan com a antagonista V_2. A més de fer un seguiment de les variables fisiològiques, s'ha estudiat el flux de sodi des de l'exterior de les criptes a l'espai pericriptal, la permeabilitat a macromolècules de les criptes de còlon distal de rata emprant dextrà 10 kDa com a traçador. Mitjançant la tècnica d'imunohistoquímica s'ha estudiat l'expressió d'ENaC, la d'-SMA i la d'AQP-2.

Resultats: Una alta concentració plasmàtica de vasopressina dóna lloc en el còlon distal a una disminució de la permeabilitat de la paret al dextrà i a un augment de la concentració pericriptal de sodi. Ambdós antagonistes dels receptors de vasopressina antagonitzen aquestes accions. En canvi, la vasopressina no té conseqüències en l'expressió de la subunitat -ENaC. Pel que respecta a la inducció de fibrosi, en els grups amb altes concentracions plasmàtiques de vasopressina l'expressió de -SMA és el doble que als grups sense vasopressina, però la presència d'aldosterona en sang aconsegueix un increment major. Tant la deshidratació com l'administració de vasopressina augmenten l'expressió d'AQP-2 en el còlon distal, acció que es veu revertida per l'administració de Tolvaptan.

Conclusió: La vasopressina intervé en la permeabilitat epitelial i en el flux de sodi a través de l'epiteli, segurament per via transcel·lular, en col·laboració amb l'aldosterona. En la fibrosi que es produeix en la zona pericriptal, la vasopressina facilita l'acció de l'aldosterona incrementant la matriu extracel·lular. S'ha confirmat la presència d'AQP-2 en la membrana apical dels colonòcits. El Tolvaptan, un antagonista específic dels receptors V_2, reverteix la inducció de la vasopressina sobre aquesta aquaporina, confirmant la implicació dels receptors V_2.

Vasopressin and crypt colon function in rats fed diets with high and low sodium content

Esther Cristià[1], Conxita Amat[1], Richard J. Naftalin[2], Miquel Moretó[1]

[1]Departament de Fisiologia, Facultat de Farmàcia, Universitat de Barcelona, Barcelona, Spain

[2] Physiology Division, King's College London, Guys Campus, London, UK

The specific role of vasopressin on colonic crypt function and its possible synergistic action with aldosterone were studied. Sprague Dawley rats fed a high-Na^+ (HS; 150 mM NaCl) or a low-Na^+ (LS; 150 µM NaCl) diet were water deprived or infused with vasopressin and some animals treated with specific V_1 and V_2 vasopressin receptor subtypes antagonists. The expression of epithelial Na^+ channel (ENaC), α-smooth muscle actin (α-SMA) and aquaporin-2 (AQP-2) were determined by immunolocalization in distal colonic mucosa. The pericryptal Na^+ concentration was determined by confocal microscopy, using a low-affinity Na^+-sensitive fluorescence dye (Sodium red) and crypt permeability was measured by the rate of escape of FITC-labeled dextran (10 kDa) from the crypt lumen into the pericryptal space in isolated rat distal colonic mucosa. High vasopressin plasma concentration raised α-SMA expression in the pericryptal sheath (P<0.05), increased the pericryptal Na^+ accumulation in this space (P<0.01) and caused a reduction of crypt wall permeability (P<0.01). All these effects were reversed by selective blocking of V_1 and V_2 receptors. No synergistic effects with aldosterone were observed. Dehydration and vasopressin infusion increased AQP-2 expression in distal colonic mucosa (P<0.05). This vasopressin action was prevented by Tolvaptan, a specific V_2 receptor antagonist (P<0.05). It is concluded that vasopressin has trophic effects in the rat distal colon, increasing pericryptal myofibroblasts growth that affects crypts absorption, and these effects are independent of the presence of aldosterone.

Key words: vasopressin – colon – permeability – fibrosis

Vasopressin (AVP), the antidiuretic hormone, plays a major role in the regulation of body water and electrolyte homeostasis. AVP acts by two different G-protein coupled receptor subtypes, V_1 and V_2 (Morel *et al*., 1992; Lolait *et al*., 1992). V_1 receptors are involved in the regulation of blood pressure and V_2 receptors are responsible for the antidiuretic effect of AVP (Nonoguchi *et al*., 1995), basically regulating aquaporin-2 (AQP-2) expression (Nielsen *et al*., 1995). AVP appears to stimulate the synthesis of AQP-2 mRNA and to regulate the insertion of AQP-2 into luminal membranes through fast exocytosis (Fushimi *et al*., 1993; Saito *et al*., 1997).

Colonic epithelium can modulate both the absorption and secretion of a variety of electrolytes and therefore has a role in water and salt homeostasis. This function may be particularly important in animals retaining a cloaca (Balment *et al*., 2006), such as fish and amphibian birds, and is regulated by many endocrine, neurocrine and paracrine agents. In earlier studies we described the role of aldosterone on crypt colon permeability and pericryptal myofibroblast growth during adaptation to a low sodium diet (Moretó *et al*., 2005; Cristià *et al*., 2005). Our results support the view that aldosterone stimulates myofibroblast growth in the distal colon crypts and this effect is responsible for both increased Na^+ absorption and decreased tissue permeability. Aldosterone increased the expression of the epithelial sodium channel (ENaC) and α-smooth muscle actin (α-SMA), increasing Na^+ accumulation in the pericryptal space and decreasing dextran permeability across the mucosa.

There is evidence that the colon could be a target of action for AVP, as it has been shown in the rat distal colon that AVP stimulates water absorption (Bridges *et al*., 1983; 1984) and AQP-2 has been found in both rat (Gallardo *et al*., 2001) and human (Mobasheri *et al*., 2005) distal colon. Vasopressin, like aldosterone, has been implicated

in extracellular matrix remodelling and growth of the heart (Harada *et al*., 1998; Goldsmith & Gheorghiade, 2005), both showing similar fibrotic effects in heart and kidney (Zannad & Radauceanu, 2005; Nagai *et al*., 2005). Similar actions of AVP and aldosterone have been described in other cases. AVP potentiates the aldosterone-mediated activation in the colon of prostasin, a membrane-bound serine protease that plays a crucial role in Na^+ transport, and of 11β-HSD2, the enzyme that inactivates glucocorticoids (Fukushima *et al*., 2004; 2005). In the kidney, AVP stimulates sodium reabsorption in renal collecting duct (Schafer & Hawk, 1992) and can exert synergistic effects with aldosterone (Hawk *et al*., 1996; Verrey, 1994). In this organ, both aldosterone and AVP can enhance ENaC expression (Machida *et al*., 2003). Moreover, both aldosterone and AVP secretion are inhibited by fluid and electrolyte homeostasis regulators such as adrenomedullin (AM) and atrial natriuretic peptide (ANP) (Nonoguchi *et al*., 1988; Szalay *et al*., 1998; Taylor & Samson, 2002).

The aim of this study was to determine a possible role of AVP on distal colon collagen formation and to clarify its role in water absorption and permeability, by determining the action of each of AVP receptors subtype to determine whether there are synergistic or similar effects between AVP and aldosterone on these actions.

Methods

Experimental Animals

Studies were performed on adult male Sprague-Dawley rats (Harlan Iberica, Barcelona, Spain) weighing 200-250 g the day of experiment. They were housed one per cage under 12:12 h light-dark cycle. The Ethical Committee for Animal Experimentation of the Universitat de Barcelona approved experimental procedures.

Experimental Protocol

*Diets***.** All animals were fed wheat and barley and had *ad libitum* access to food throughout the experiments. Sodium content was given in drinking water: the high sodium diet (HS) had 150 mM NaCl meanwhile the low sodium diet (LS) 150 μM NaCl. The HS groups were fed this diet during 7 days. To study a low sodium adaptation, after 4 days of HS, the LS groups were changed to the LS for 3 days.

*AVP Study***.** Two strategies were used to increase plasma AVP concentration: 24h water restriction and AVP infusion. Animals on either HS or LS diets were deprived of water for 24 h. the last day of the experiment, these were named as HSD and LSD groups. Osmotic minipumps (model 2002, Alzet, Palo Alto, CA) filled with AVP (Sigma) dissolved in saline, were implanted subcutaneously in the neck in both HS and LS rats. AVP was delivered at a rate of 1 $ng \cdot kg^{-1} \cdot min^{-1}$ for 3 days. To inhibit the production of aldosterone and angiotensin II, some LS rats received the angiotensin converting enzyme (ACE) inhibitor, captopril (CAP, Sigma) administered in drinking water at a dose of 65 $mg \cdot kg^{-1} \cdot day^{-1}$ for 3 days. Moreover, some animals were treated with AVP receptors antagonists. Manning Peptide (d(CH2)51Tyr(Me)2Arg8)-Vasopressin, Sigma), a V_1 receptor (VR1) antagonist was administered at 1 $\mu g \cdot kg^{-1}$ i.p. for 3 days. Tolvaptan (OPC-41061, gift from Otsuka Pharmaceutical Co, Japan), a V_2 receptor (VR2) inhibitor was used at a dose of 5 $mg \cdot kg^{-1}$ for 3 days, dissolved in 1% hydroxypropylmethylcellulose (HPMC, Sigma) as described by Yamamura *et al*. (1998). A summary of all groups with their plasma hormonal profiles is shown in Table 1.

Table 1. Experimental groups and their hormonal profiles

GROUP	Aldosterone	Vasopressin
HS	↓	↓
HSD	↓	↑
HS+AVP	↓	↑
HS+AVP+VR2	↓	↑
LS	↑	↓
LSD	↑	↑
LSD+CAP	↓	↑
LSD+CAP+VR1	↓	↑
LSD+CAP+VR2	↓	↑
LSD+AVP+CAP	↓	↑

*Tissue preparation***.** Rats were maintained in metabolic cages during the last three days, and 24-h urinary output, water intake, food consumption and weight changes were measured daily. Urinary volume, osmolality and Na^+, K^+ and AVP concentration were also measured. To prevent urinary bacterial growth, azlocillin (Sigma) was added to the collection tube. Thereafter, rats were anaesthetized with ketamine/xylacine (100/10 $mg \cdot kg^{-1}$) i.p.; the descending colon was removed rapidly and the contents removed by washing with PBS. Colonic mucosa was isolated from the muscularis mucosae by scraping with a glass slide and maintained in Earl's medium for its use in *in*

vitro functional studies (pericryptal Na^+ accumulation, dextran permeability), or fixed in 4% paraformaldehyde in PBS at 4ºC for 24 h for immunohistochemistry studies. Trunk blood was collected in tubes containing EDTA (1.5 $mg \cdot ml^{-1}$ of blood) and a protease inhibitor cocktail (Sigma) and kept on ice until centrifugation at 4ºC. Plasma was aliquoted and stored at –80ºC for subsequent assay of plasma aldosterone and ion concentrations.

Hormone and ions determinations

Hormones were determined by RIA using commercially available kits: Aldosterone RIA kit Immunotech (France) for plasma aldosterone and RIA I125 Bühlmann Laboratories (Switzerland) for urine vasopressin. Plasma Na^+ and K^+ concentrations were measured using potentiometric direct dry chemistry (Beckman Coulter Corporation, USA). Their urinary concentrations were determined using inductively coupled plasma optical emission spectroscopy (ICP-OES Thermo Jarrell Ash model ICAP 61E, Genesis Laboratories Systems Inc., Colorado, USA).

Immunocytochemistry

Colonic mucosal tissues (0.5 cm^2 pieces) were stained according to the following protocol. The procedure was the same for all antibodies used. Tissues were permeabilized in 0.2% Triton X-100 in blocking buffer (1% BSA in PBS and glycine) for 30 min. Samples were washed three times in PBS and incubated for 90 min with primary antibody (1:100 for ENaC and α-SMA, 1:50 for AQP-2). The antibodies used were monoclonal anti-α-SMA clone IA4 and rabbit anti-water channel AQP-2 from Sigma, and rabbit anti-rat γ-ENaC antibody from Alpha Diagnostics Intl. Inc., San Antonio, USA. After a 3x wash in PBS, tissues were incubated for 60 min in each secondary antibody (1:100). Both secondary antibodies were purchased from Molecular Probes (Eugene, OR), anti-αSMA staining Texas Red goat anti-mouse IgG and anti-rabbit Alexa-488 antibody for ENaC and AQP-2. Finally, tissues were washed again 3x in PBS.

Pericryptal Na^+ accumulation

Na^+ concentration in isolated rat distal colonic mucosa was determined as described earlier (Moretó *et al*., 2005) using a modification of a dual wavelength laser scanning confocal microscopic method in which low affinity Na^+-sensitive dye (Sodium Red, and BODIPY-fl) is bound to microscopic polystyrene beads (Jayaraman *et al*., 2001). Briefly, colonic mucosal pieces were loaded with the dye containing beads and seen in confocal microscopy. The local Na^+ concentration was estimated by ratiometric imaging of the beads using the Na^+ red signal which increases linearly in the concentration range 0-500 mM and the green signal from BODIPY-fl.

Dextran permeability

Crypt permeability to dextran was monitored by the rate of escape of fluorescein isothiocyanate (FITC) labeled dextran (molecular weight 10000, FITC dextran; Sigma Chemicals, St Louis, MI) from the crypt lumen into the pericryptal space at 37ºC. Crypt luminal and pericryptal concentration of FITC-dextran was estimated by monitoring the ratio of fluorescence intensity of each zone. The procedures performed were as described earlier (Naftalin *et al*., 1999; Moretó *et al*., 2005).

Confocal images

Each piece of tissue was viewed from the mucosal side with the confocal microscope using 20x or 40x Leica SPII oil immersion lens. The focus plane was taken to the surface of the tissue and images were captured at 2.5 µm or 5 µm steps using the automatic Z-step motor. Images were taken from 0 µm down to 40 µm below the surface. With dextran permeability the scans were repeated at 5 min intervals for 20 min. For Na^+ red ratio imaging, the tissues were pre-incubated at 37ºC in a humidified hood for 30 min with the dye prior to viewing with the confocal microscope. This allows the dye beads to penetrate into the pericryptal and interstitial spaces. The captured images represent the general level of staining throughout the whole tissue and were obtained with the same optical conditions, gain and section size.

Image analysis

The captured images were analyzed using the program Image J (Image J 1.32, http://rsb.info.nih.gov/ij) to quantify the fluorescence from each antibody (Abramoff *et al*., 2004). The fluorescence was quantified by areas, which were divided into either crypt or inter-crypt and were taken by selecting a region of interest within the relevant part of the image. Three areas of both crypt and inter-crypt regions were taken for image analyses and therefore there were thirty

measurements per tissue at the various depths. The mean and SEM of the measurements after background subtraction from each image was calculated. To obtain averaged fluorescence intensities within the crypt lumen and pericryptal sheath projected images using maximal intensity averaging over the depths 5-30 µm were obtained for each rat and results compared for each condition. For the Na^+ ratio analysis, image pairs of sodium red and BODIPY-fl were acquired from the same field. Background images were obtained under the same conditions, but without loading with the dye. Ratio images (red-to-green fluorescence) were obtained by pixel-by-pixel division of background-subtracted images. Background values were <10% of signal. Averaged ratios were obtained by integration of red and green fluorescence intensities over specified regions of interest.

Statistical analyses

Data were expressed as means ± SEM. Comparisons between groups were made by ANOVA using SPSS-10.0 software (SPSS) followed by Scheffé's *post-hoc* test. Three different effects were analyzed: dietary effect (HS *vs* LS), AVP effect (AVP infused and water deprived groups *vs* HS and LS) and the antagonists effects (VR1 and VR2 *vs* AVP). In the case of plasma aldosterone concentrations, Captopril effect was analyzed *vs* the LS group. Differences were considered statistically significant when the test yielded $P<0.05$.

Results

Physiological data

All physiological findings indicated both the consistency and efficacy of dietary and pharmacological treatments. Fig. 1 shows the 24 h water and urine excretion during the three days in the metabolic cages, where an appreciable antidiuretic effect of AVP was observed. Total water intake was reduced by AVP administration (HS+AVP and LS+AVP+CAP groups) but this effect was prevented by the V_2 receptor antagonist. Urine excretion was reduced in groups with high plasma AVP concentration, resulting from 24h water deprivation and AVP infusion. Both receptor antagonists prevented the antidiuretic AVP effect on urine excretion.

Table 2. Physiological data for control and water deprived groups

	Urine Osmolality (mosm/kg)	Hematocrit (%)	Plasma osmolality (mosm/kg)
HS	1171 ± 149 (8)	42.3 ± 0.36 (5)	288 ± 6.6 (5)
HSD	1668 ± 230 (8)*	45.5 ± 0.72 (6)*	316 ± 3.7 (5)*
LS	894 ± 153 (7)$^{\varphi}$	43.3 ± 0.10 (5)	286 ± 6.4 (5)
LSD	1680 ± 222 (8)*	45.9 ± 0.68 (5)*	319 ± 3.2 (6)*
LSD+CAP	1466 ± 145 (7)*	45.8 ± 0.62 (6)*	314 ± 6.2 (6)*
LSD+CAP+VR1	918 ± 67 (8)$^{\#}$	45.9 ± 0.31 (5)*	315 ± 6.9 (5)*
LSD+CAP+VR2	871 ± 71 (8)$^{\#}$	45.7 ± 0.43 (8)*	314 ± 2.1 (5)*

Urine and plasma osmolality and hematocrit data from control (HS and LS) and 24h water deprived (D) groups the last day of diet. Values are means ± SEM (n= number of rats). $^{\varphi}P < 0.05$ LS *vs* HS; *$P < 0.05$ Control *vs* dehydration; $^{\#}P<0.05$ Antagonist effect.

The effect of 24h water deprivation on urine osmolality, hematocrit and plasma osmolality is shown in Table 2. The effects on plasma osmolality and hematocrit were consistent with dehydration; both being significantly increased after 24h water deprivation. The urine osmolality, urine excretion rate and vasopressin measurements were also consistent with dehydration, and similar to those reported previously (Desai *et al*., 2005; Gottlieb *et al*., 2006). Urine osmolality increased after 24h water deprivation but in both VR1 and VR2 groups the receptor antagonists reversed the antidiuretic response to AVP.

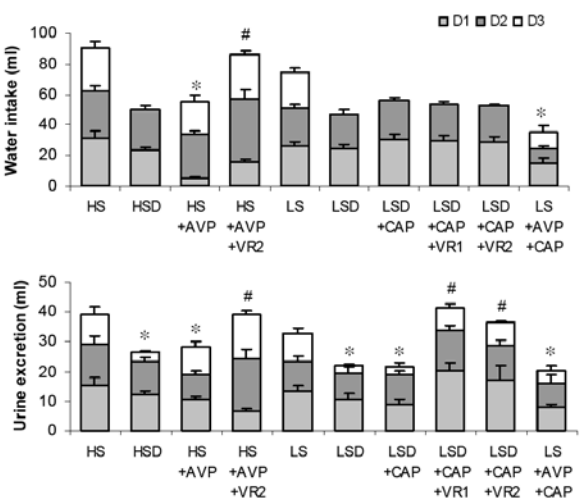

Figure 1. Water intake and Urine excretion

The 24h daily water intake and urine excretion during the last three days of diet, when rats were in metabolic cages, for all experimental groups. Control groups: HS (high sodium diet) and LS (low sodium diet); "D" groups were 24h water deprived; "AVP" were infused with AVP during 7 days; "VR1" rats were treated with a V1 receptor antagonist; "VR2" rats were treated with a V2 receptor antagonist; "CAP" rats were treated with captopril. Values are means ± SEM (n=7-11 rats). *$P < 0.05$ Control *vs* AVP; $^{\#}P < 0.05$ Antagonist *vs* AVP

Table 3. Hormone and ion determinations for all experimental groups

	Aldosterone plasma (nM)	Vasopressin urine (pg/ml)	Urinary Na^+ (mmol, 3 days)	Urinary K^+ (mmol, 3 days)	Na^+ plasma at day 3 (mM)	K^+ plasma at day 3 (mM)
HS	0.15 ± 0.03 (7)	1.87 ± 0.40 (6)	9.63 ± 0.57 (7)	3.01 ± 0.07 (7)	141 ± 1.05 (7)	5.38 ± 0.22 (7)
HSD	0.45 ± 0.14 (5)	45.2 ± 2.1 (5)*	5.65 ± 0.57 (6)*	3.65 ± 0.26 (6)	144 ± 1.4 (6)	5.05 ± 0.20 (6)
HS+AVP	0.18 ± 0.03 (5)	123 ± 21 (5)*	5.44 ± 0.58 (4)*	2.83 ± 0.14 (4)	146 ± 2.1 (5)	4.82 ± 0.22 (5)
HS+AVP+VR2	0.26 ± 0.08 (5)	132 ± 33 (5)*	9.68 ± 0.54 (4)$^{\#}$	2.75 ± 0.06 (4)	142 ± 2.4 (5)	4.98 ± 0.27 (5)
LS	1.4 ± 0.29 (7)$^{\varphi}$	2.05 ± 0.41 (6)	0.31 ± 0.06 (7)$^{\varphi}$	2.71 ± 0.22 (7)	142 ± 2.1 (6)	5.29 ± 0.15 (6)
LSD	1.2 ± 0.42 (6)$^{\varphi}$	42.4 ± 2.7 (5)*	0.34 ± 0.06 (6)$^{\varphi}$	2.98 ± 0.18 (6)	145 ± 2.4 (8)	5.07 ± 0.10 (8)
LSD+CAP	0.04 ± 0.01 (6)$^{¥}$	47.6 ± 7.0 (5)*	0.64 ± 0.05 (8)$^{¥}$	3.10 ± 0.35 (8)	141 ± 0.9 (8)	5.04 ± 0.09 (8)
LSD+CAP+VR1	0.22 ± 0.07 (6)$^{¥}$	39.8 ± 2.3 (5)*	0.83 ± 0.10 (8)$^{¥}$	3.21 ± 0.16 (8)	140 ± 0.9 (8)	5.21 ± 0.15 (8)
LSD+CAP+VR2	0.14 ± 0.05 (6)$^{¥}$	43.0 ± 5.3 (5)*	0.86 ± 0.09 (8)$^{¥}$	2.67 ± 0.23 (8)	143 ± 1.8 (8)	5.12 ± 0.19 (8)
LS+AVP+CAP	0.23 ± 0.12 (5)$^{¥}$	153 ± 41 (5)*	2.24 ± 0.09 (4)$^{¥}$	2.16 ± 0.09 (4)	140 ± 2.9 (4)	4.93 ± 0.07 (4)

Plasma aldosterone and Na^+ and K^+ and urinary vasopressin and Na^+ and K^+ were determined. Control groups: HS (high sodium diet) and LS (low sodium diet); "D" groups were 24h water deprived; "AVP" were infused with AVP during 7 days; "VR1" rats were treated with a V1 receptor antagonist; "VR2" rats were treated with a V2 receptor antagonist; "CAP" rats were treated with captopril. "3 days" means the sum of the ion excreted during the 3 days in metabolic cages; "At day 3" means the quantification the last day in the metabolic cage. Values are means ± SEM (n= number of rats). $^{\varphi}P < 0.01$ LS *vs* HS; $^{*}P < 0.05$ Control *vs* D and AVP; $^{\#}P < 0.05$ Antagonist effect; $^{¥}P < 0.01$ Captopril effect

Hormonal and Na^+ and K^+ determinations in the treatment groups are shown in Table 3. AVP excretion was significantly increased after both water deprivation and AVP infusion (P<0.01). Dietary NaCl intake had no effect on AVP plasma concentration. The plasma aldosterone concentration in LS groups was much higher than in HS groups. The HS condition is well suited to independent study of AVP action, as aldosterone levels are very low. The animals fed the LS diet, either with normal hydration or water deprived (LSD), had similar plasma aldosterone concentrations. CAP administration to LS animals lowered plasma aldosterone concentration (P<0.01) and resulted in an increased Na^+ excretion, as expected. The V_2 receptor antagonist prevented the reduction in Na^+ excretion induced by AVP in the HS conditions. Plasma Na^+ concentration was maintained in the physiological range in all experimental groups.

AVP effect on pericryptal myofibroblasts

The effect of AVP on pericryptal myofibroblasts growth was studied by looking to α-SMA expression, as it is the protein used to identify myofibroblasts (Jain *et al*., 1998). As reported previously, during the transition from a HS to a LS diet myofibroblasts surrounding colonic crypts proliferate (LS and LSD groups *vs* HS, P<0.01; Fig. 2) and this effect was ascribed to aldosterone (Cristià *et al*., 2005). In this new series of experiments, the presence of high AVP levels increases by 2-fold the α-SMA expression *vs* the control HS (P<0.05) in both HS and LS diets (HSD, HS+AVP, LSD+CAP and LS+AVP+CAP groups). In the absence of aldosterone, the action of AVP on α-SMA expression although less than that observed with aldosterone alone (LS) or with both aldosterone and vasopressin together (LSD), where the increase is 4-fold higher, is still 2-fold higher than in the HS group (Fig. 2). The effect of AVP on α-SMA expression was confirmed with AVP receptor antagonists, which prevented the AVP-induced increase in α-SMA. Thus, both receptor types, V_1 and V_2, are implicated in this trophic stimulation.

The pericryptal sheath myofibroblasts create a barrier to diffusion behind which Na^+ accumulates. Thus, quantification of pericryptal Na^+ accumulation is an indirect measurement of myofibroblast barrier function and development. Significant differences were obtained in pericryptal Na^+ accumulation between all the LS groups and the HS group (P<0.01), being higher in the LS condition. In groups with high plasma concentration of AVP and low or absent aldosterone (HSD, HS+AVP, LSD+CAP, LS+AVP+CAP), Na^+ accumulation in the pericryptal space was greatly increased. Raised pericryptal Na^+ was also found in the LSD group, where both plasma aldosterone and vasopressin concentrations were high, but no synergistic effects were observed. Administration of the two AVP receptor antagonists prevented pericryptal Na^+ accumulation, with similar values to those observed in the HS group. Pericryptal Na^+ concentration for each group can be seen in Fig. 3A.

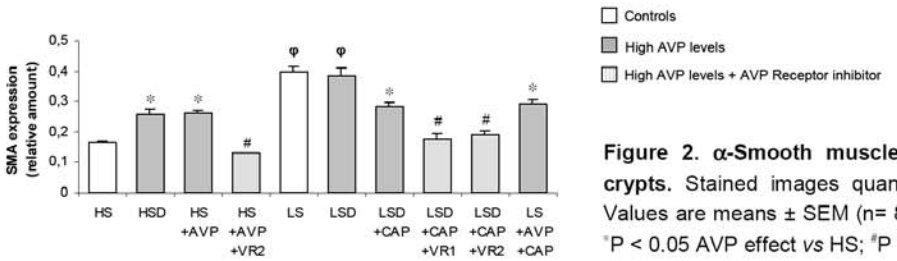

Figure 2. α-Smooth muscle actin expression in colonic crypts. Stained images quantification of α-SMA expression. Values are means ± SEM (n= 8-12 crypts). $^{\varphi}P < 0.01$ LS *vs* HS $^{*}P < 0.05$ AVP effect *vs* HS; $^{\#}P < 0.05$ Antagonist effect

AVP effect on Colonic Permeability and Transport

The dextran permeability of the crypt wall was measured by the rate of escape of FITC-labelled dextran (10kDa) from the crypt lumen into the pericryptal space. Dextran permeability between the crypt lumen and the pericryptal space is an indicator of paracellular permeability of the crypt epithelium and it is also a reflection of the permeability of the pericryptal sheath (Thiagarajah *et al*., 2001a, 2001b). In the HS condition, aldosterone perfusion converted the leaky colon (typical of the HS condition) into a tight tissue (Moretó *et al*., 2005). In the present series, vasopressin had similar effects to aldosterone in reducing dextran permeability. AVP perfused groups, without aldosterone, had similar dextran permeabilities as in the LS or LSD conditions, where aldosterone was present, and were significantly different from the HS group ($P<0.01$). Both receptor antagonists subtypes reversed the AVP action on dextran permeability making them leakier to dextran.

The effect of AVP on the capacity to take up Na^+ was studied by quantification of γENaC subunit expression. The γENaC subunit was strongly induced in the distal colon in the LS diet, when aldosterone was present (LS and LSD) ($P<0.01$; Fig. 4). However, when the LSD group was treated with CAP to inhibit aldosterone synthesis, the rise in the channel expression was abrogated. Similarly, none of the other groups with high plasma AVP concentration, and without aldosterone, showed an increase in γENaC immunohistochemical staining, indicating that ENaC expression in the distal colon is independent of AVP levels.

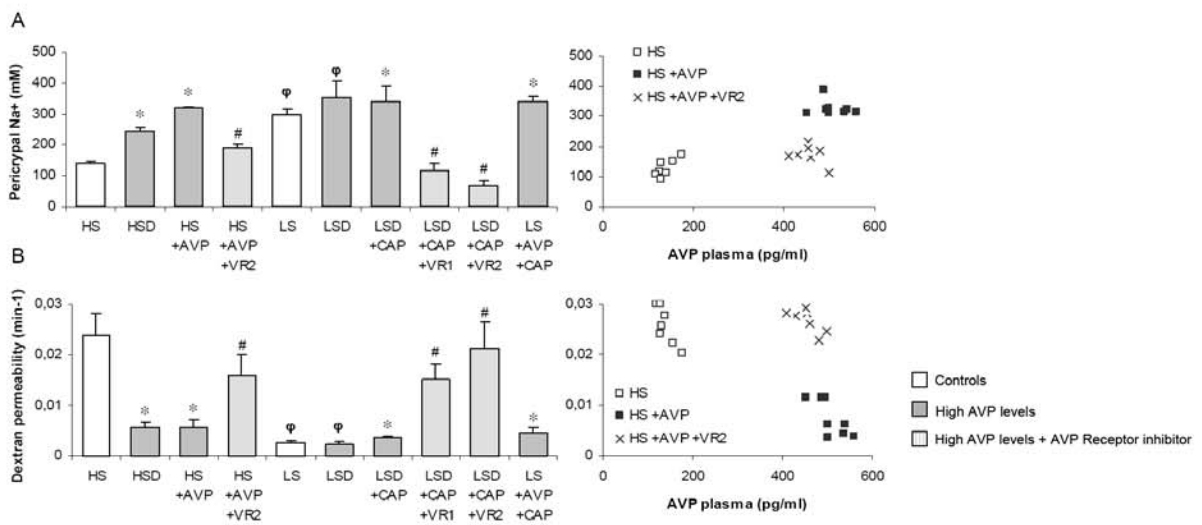

Figure 3. Pericryptal sodium accumulation and dextran permeability

A) Quantification of Na^+ accumulation in the pericryptal space in all experimental groups; Pericryptal Na^+ *vs* AVP concentration in HS, HS+AVP and HS+AVP+VR2 groups. B) Dextran permeability in all experimental groups; Dextran permeability *vs* AVP concentration in HS, HS+AVP and HS+AVP+VR2 groups. Values are means ± SEM (n= 8-12 crypts). $^{\varphi}P < 0.01$ LS *vs* HS $^{*}P < 0.01$ AVP effect; $^{\#}P < 0.01$ Antagonist effect

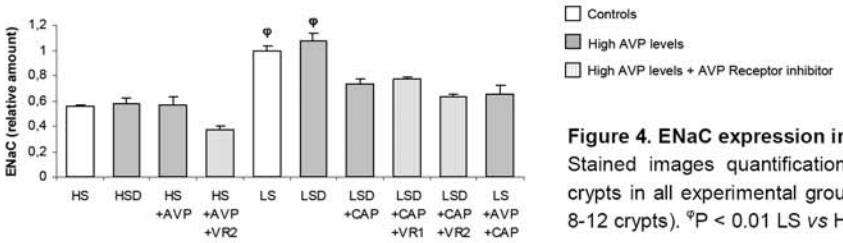

Figure 4. ENaC expression in colonic crypts
Stained images quantification of ENaC expression in colonic crypts in all experimental groups. Values are means ± SEM (n= 8-12 crypts). $^{\Phi}P < 0.01$ LS *vs* HS

AVP effect on AQP-2 Expression

The amount of AQP-2 was quantified by using confocal imaging of the fluorescence. These results showed that both dehydration and AVP infusion increased AQP-2 expression in colonic distal mucosa (Fig. 5). Immunohistochemical staining of AQP-2 was only seen in the mucosal surface, not inside the crypt. Aldosterone did not affect AQP-2 expression, as the LS group did not show any staining. The VR2 antagonist Tolvaptan prevented the stimulatory effect of AVP on AQP-2 expression in both HS and LS groups, showing the implication of V_2 receptors in this AVP action. The VR1 antagonist was ineffective in reducing AVP-induced effects on AQP-2 expression. A selection of representative confocal images is shown in Fig. 7.

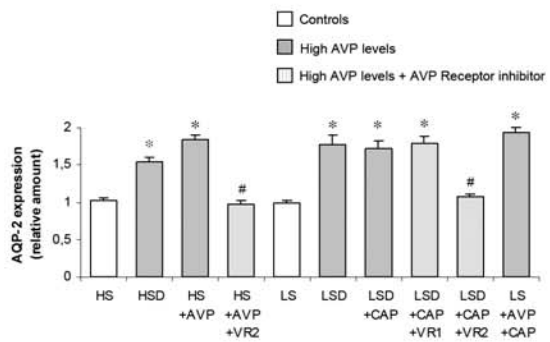

Figure 5. Aquaporin-2 expression in colonic mucosa
Stained images quantification of AQP-2 expression in colonic mucosa in all experimental groups. Values are means ± SEM (n=9-12 crypts). $^{*}P < 0.05$ AVP effect; $^{\#}P < 0.05$ Antagonist effect

Discussion

The effects of AVP on colonic crypt function have been studied in rats fed a diet containing either a high NaCl (HS) or a very low NaCl (LS) in order to explore further the role of this hormone in the physiological adaptations to LS intake (Naftalin & Pedley, 1999; Moretó *et al*., 2005). These new findings indicate the action of aldosterone and AVP are complementary.

By monitoring pericryptal myofibroblast growth, Na^+ accumulation in the pericryptal sheath, dextran permeability and ENaC and AQP-2 expression in colonocytes we obtained a broad view of the interrelated factors regulating the transport and permeability properties of the crypt wall. Proliferation of the pericryptal myofibroblast layer is illustrated by enhanced α-SMA expression. It appears that AVP can mimic aldosterone action in stimulating myofibroblasts growth as α-SMA expression is raised through V_1 and V_2 receptors. This trophic effect of AVP was corroborated by monitoring Na^+ accumulation in the pericryptal sheath and dextran permeability. Vasopressin enhances Na^+ accumulation in the pericryptal sheath and creates a hyperosmotic gradient across the crypt wall similar to that induced by aldosterone (Moretó *et al*., 2005). The growth of the myofibroblast layer also produced an accumulation of dextran in the pericryptal sheath resulting in a decrease in dextran permeability across the crypt wall. These effects cannot be ascribed to aldosterone action, since its plasma concentration in the groups with high plasma AVP concentration was very low, except in the LSD condition, where a complementary effect of both hormones is observed. It seems, therefore, that AVP and aldosterone have similar effects in modulating pericryptal myofibroblast growth.

Trophic effects of vasopressin on the extracellular matrix have been previously observed. Harada *et al*. (1998) reported that chronic vasopressin infusion in rats caused a significant increase in TGF-β1 and its mRNA expression in kidney. TGF-β1 increases extracellular matrix by stimulating the production of collagen and non-collagenous protein components and by inhibiting their degradation (Roberts *et al*.,

1986; Campbell & Katwa, 1997, Thiagarajah *et al.*, 2002). Moreover, patients with heart failure had significantly higher plasma concentration of vasopressin compared with control groups (Sanghi *et al.*, 2005), suggesting that AVP may be involved in glomerular proliferation and in the expansion of the mesangial matrix *in vivo*; thus playing an important role in the pathophysiology of the heart failure syndrome. In rats, AVP has been shown to stimulate myocardial cell hypertrophy, an action that shares many of the features seen in the typical hypertrophy response of the adult heart to other hormones, such as aldosterone or angiotensin II (Tahara *et al.*, 1998). In the heart, both AVP receptors are involved in organ remodelling (Goldsmith & Gheorghiade, 2005). The stimulation of V_1 receptors is thought to contribute directly to myocardial hypertrophy and aggravate adverse remodelling. The stimulation of V_2 receptors may contribute to increased cardiac preload which, in turn, exacerbates diastolic wall stress which worsens eccentric remodelling. Our experiments show that both receptors are implicated in the trophic effects of vasopressin in the distal colon as both specific receptors antagonists prevent AVP effects.

The increase in Na^+ accumulation in the pericryptal space implies an increase in Na^+ transport and for this reason the expression of ENaC was studied. Paradoxically, AVP does not enhance ENaC expression in the distal colonic apical membranes. Hormonal regulation of ENaC varies between organs and tissues (Stokes & Sigmund, 1998). In the kidney, both aldosterone and AVP have a role in enhancing ENaC expression but in the distal colon only aldosterone is involved (Machida *et al.*, 2003). Infusion of dDAVP, a selective V_2 receptor agonist, did not modify mRNA expression of any ENaC subunit in the distal colon (Nicco *et al.*, 2001). Another study suggests that vasopressin inhibition of electrogenic Na^+ absorption depends mainly on V_1 receptor activation (Sato *et al.*, 1999). Our results show that in the LSD group (with high levels of aldosterone and vasopressin), ENaC expression is similar to the LS group (with high aldosterone and low AVP levels). This suggests that AVP does not enhance the effects of aldosterone on ENaC expression. Aldosterone alone suffices to up-regulate ENaC expression in the distal colon. Thus, in the colon, vasopressin does seem not to control Na^+ transport via the transcellular route but may modulate passive and paracellular Na^+ transport and thereby increase the capacity of the tissue to maintain a high Na^+ gradient across the crypt wall.

Both water deprivation (Nielsen *et al.*, 1995; Kishore *et al.*, 2005) and vasopressin stimulation (Kishore *et al.*, 1996; Terris *et al.*, 1996) increase AQP-2 expression in the kidney, an effect mediated by the V_2-type basolateral receptors. AVP regulates AQP-2, acutely controlling intracellular AQP-2 trafficking (Nielsen *et al.*, 1995; Noda & Sasaki, 2005). A slower effect at transcriptional level has been observed in rats after 24h of water restriction (DiGiovanni *et al.*, 1994; Saito *et al.*, 1997). Gallardo *et al.* (2001) were the first to observe the presence of AQP-2 in the dehydrated rat colon. They suggested that AQP-2 could provide an apical membrane route for regulated transepithelial water transport in the colon as they showed that water absorption in the distal colon is increased in water deprivation and inhibited by aquaporin blockade.

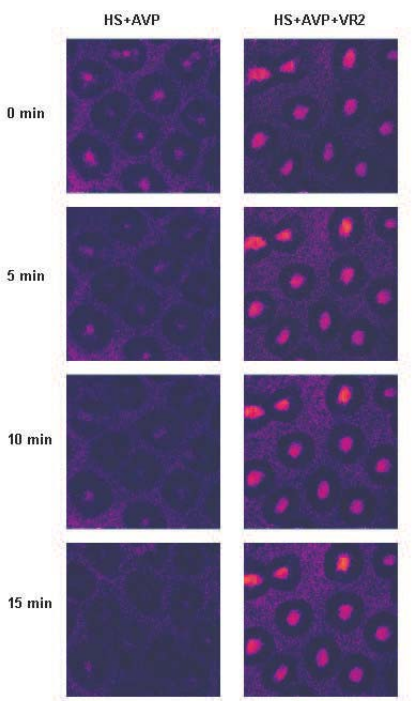

Figure 6. Illustration of dextran permeability in colonic crypts
Images show dextran permeation across crypt wall into interstitial space along the time. Dextran 10 kDa is more permeable across HS+AVP+VR2 crypts than HS+AVP crypts, showing AVP effect reducing dextran permeability. Images were taken at 10 µm from surface.

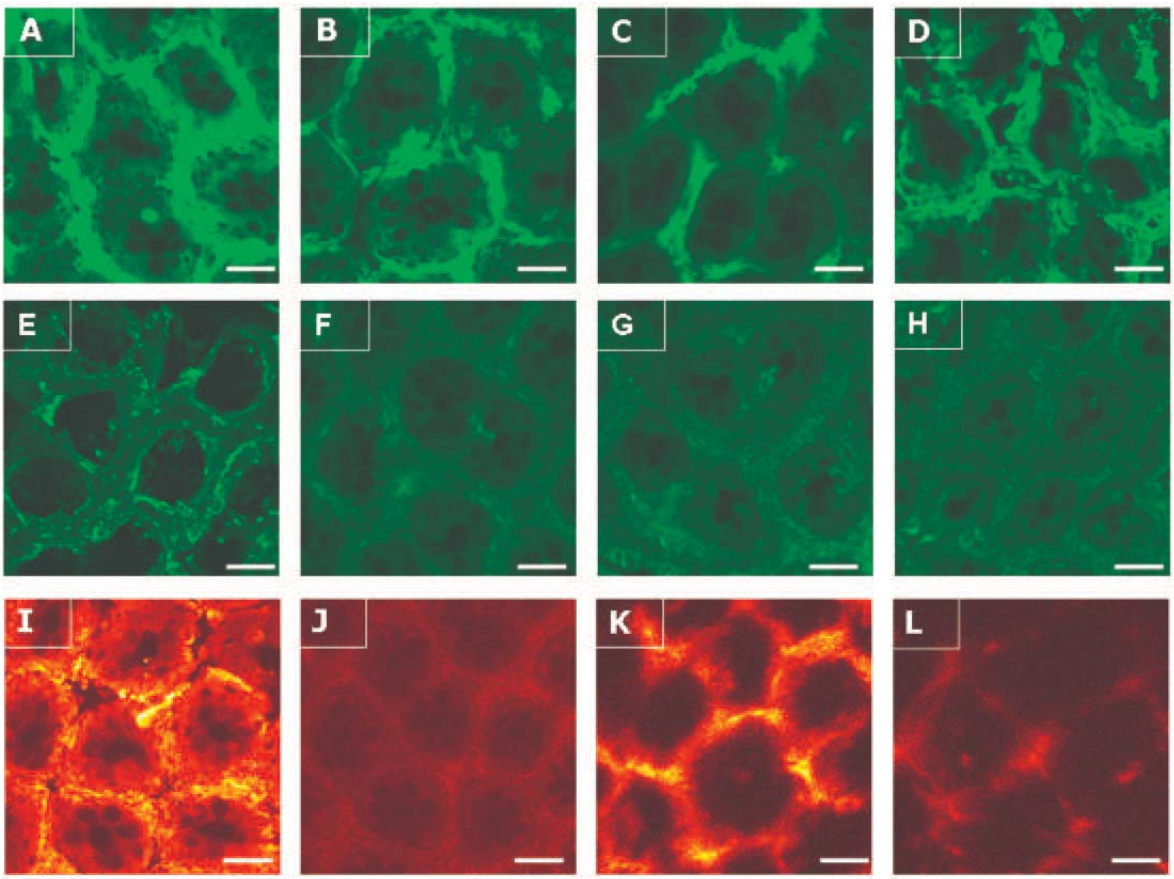

Figure 7. Confocal images of α-SMA and AQP-2 staining in colonic crypts
From A to H, each image belongs to a different experimental group with different hormonal profile showing the effects of aldosterone and vasopressin in α-SMA expression. A) LSD, with high aldosterone and vasopressin plasmatic levels; B, C and D, correspond to groups with a high plasmatic vasopressin concentration without aldosterone; B) HSD; C) LSD+AVP+CAP; D)HS+AVP; E) HS, low levels of aldosterone and vasopressin; F) LSD+CAP+VR1, high vasopressin levels but with the treatment of a selective V_1 receptor antagonist; G and H belong to groups with high vasopressin levels with a selective V_2 receptor antagonist; G) LSD+CAP+VR2; H) HS+AVP+VR2. From I to L, they are images of AQP-2 staining. In I (LSD group) and K (HS+AVP group) images increased AQP-2 expression due to raised vasopressin. In J (LSD+VR2 group) and L (HS+AVP+VR2 group) it can be seen Tolvaptan antagonist action. All images were taken at a depth of 20 µm from the tissue surface.

Our results confirm that dehydration enhances colonic expression of AQP-2 and demonstrate that this is a direct response to AVP infusion. AQP-2 is expressed only on the surface mucosa, with a similar distribution to that described by Gallardo *et al*. (2001) who found AQP-2 protein only in the apical membrane of columnar absorptive cells of the mucosal surface, although the AQP-2 mRNA was mainly found in crypt epithelial colonocytes. As with kidney (Hayashi *et al*., 1996), the AVP effect on AQP-2 regulation in the colon is a response to V_2 receptor activation. This is corroborated by our finding that Tolvaptan prevents colonic aquaporin expression (Fig. 7).

The dual effects of vasopressin in the distal colon in stimulating myofibroblast growth and increasing AQP2 are consistent with its antidiuretic role. In the distal colon water is removed from luminal faeces both by the surface mucosa which can exert very little suction tension but has a high transport capacity whereas crypts have a low water transport capacity but can exert a high tension (Bleakman & Naftalin 1990; McKie *et al*., 1990; Zammit *et al*., 1994). One of the roles attributed to pericryptal sheath myofibroblasts in distal colon is to maintain a hypertonic NaCl concentration in pericryptal space. This generates the large hydraulic tension within the crypt lumen needed to dehydrate faeces (Naftalin, 2004). Vasopressin could facilitate water absorption in the distal colon by two mechanisms, by stimulating myofibroblast

growth, pericryptal NaCl hypertonicity is enhanced by retarding NaCl leakage into the submucosa, and by regulating AQP-2 expression in the apical membrane increased rates of fluid are absorbed from watery faeces.

These results clarify the mechanisms of regulation of colonic function and show that aldosterone and vasopressin induce trophic responses that are also observed in pathological alterations of kidney and heart. This suggests that the colon can be used as a model to explore the mechanisms involved in the regulation of myofibroblast growth.

References

Abramoff MD, Magelhaes PJ & Ram SJ (2004). Image Processing with ImageJ. *Biophotonics Int* 11, 36-42.

Balment RJ, Lu W, Weybourne E & Warne JM (2006). Arginine vasotocin a key hormone in fish physiology and behaviour: a review with insights from mammalian models. *Gen Comp Endocr* 147, 9-16.

Bleakman D & Naftalin RJ (1990). Hypertonic fluid absorption from rabbit descending colon in vitro. *Am J Physiol* 258, G377-390.

Bridges RJ, Nell G & Rummel W (1983). Influence of vasopressin and calcium on electrolyte transport across isolated colon from normal and dexamethasone-treated rats. *J Physiol* 338, 463-475.

Bridges RJ, Rummel W & Wollenberg P (1984). Effects of vasopressin on electrolyte transport across isolated colon from normal and dexamethasone-treated rats. *J Physiol* 355, 11-23.

Campbell SE & Katwa LC (1997). Angiotensin II stimulated expression of transforming growth factor-beta 1 in cardiac fibroblasts and myofibroblasts. *J Mol Cell Cardiol* 29, 1947-1958.

Cristià E, Afzal-Ahmed I, Pérez-Bosque A, Amat C, Naftalin RJ & Moretó M (2005). Pericryptal myofibroblast growth in rat descending colon induced by low-sodium diets is mediated by aldosterone and not by angiotensin II. *J Membrane Biol* 206, 53-59.

Desai M, Gayle D, Kallichanda N & Ross MG (2005). Gender specificity of programmed plasma hypertonicity and hemoconcentration in adult offspring of water-restricted rat dams. *J Soc Synecol Investig* 12, 409-415.

DiGiovanni SR, Nielsen S, Christensen EI & Knepper MA (1994). Regulation of collecting duct water channel expression by vasopressin in Brattleboro rat. *Proc Natl Acad Sci USA* 91, 8984-8988.

Fukushima K, Naito H, Funayama Y, Yonezawa H, Haneda S, Shibata C & Sasaki I (2004). In vivo induction of prostasin mRNA in colonic epithelial cells by dietary sodium depletion and aldosterone infusion in rats. *J Gastroenterol* 39, 940-947.

Fukushima K, Funayama Y, Yonezawa H, Takahashi K, Haneda S, Suzuki T, Sasano H, Naito H, Shibata C, Krozowski ZS & Sasaki I (2005). Aldosterone enhances 11beta-hydroxysteroid dehydrogenase type 2 expression in colonic epithelial cells in vivo. *Scand J Gastroenterol* 40, 850-857.

Fushimi K, Uchida S, Hara Y, Hirata Y, Marumo F & Sasaki S (1993). Cloning and expression of apical membrane water channel of rat kidney collecting tubule. *Nature* 361, 549-552.

Gallardo P, Cid LP, Vio CP & Sepulveda F (2001). Aquaporin-2, a regulated water channel, is expressed in apical membranes of rat distal colon epithelium. *Am J Physiol Gastrointest Liver Physiol* 281, G856-G863.

Goldsmith SR & Gheorghiade M (2005). Vasopressin antagonism in heart failure. *J Am Coll Cardiol* 46, 1785-1791.

Gottlieb HB, Ji LL, Jones H, Penny ML, Fleming T & Cunningham JT (2006). Differential effects of water and saline intake on water deprivation-induced c-Fos staining in the rat. *Am J Physiol Regul Integr Comp Physiol* 290, R1251-R1261.

Harada K, Ogura T, Yamauchi T, Otsuka F, Mimura Y, Hashimoto M, Oishi T & Makino H (1998). Effect of continuous infusion of vasopressin on glomerular growth response in spontaneously hypertensive rats. *Regul Pept* 74, 11-18.

Hawk CT, Li L & Schafer JA (1996). AVP and aldosterone at physiological concentrations have synergistic effects on Na^+ transport in rat CCD. *Kidney Int Suppl* 57, S35-S41.

Hayashi M, Sasaki S, Tsuganezawa H, Monkawa T, Kitajima W, Konishi K, Fushimi K, Marumo F & Saruta T (1996). Role of vasopressin V2

receptor in acute regulation of aquaporin-2. *Kidney Blood Press Res* 19, 32-7.

Jain MK, Layne MD, Watanabe M, Chin MT, Feinberg MW, Sibinga NE, Hsieh CM, Yet SF, Stemple DL & Lee ME (1998). In vitro system for differentiating pluripotent neural crest cells into smooth muscle cells. *J Biol Chem* 273, 5993-5996.

Jayaraman S, Song Y, Vetrivel L, Shankar L & Verkman AS (2001). Non-invasive fluorescence measurement of salt concentration in the airway surface liquid. *J Clin Invest* 107, 317-324.

Kishore BK, Terris JM & Knepper MA (1996). Quantitation of aquaporin-2 abundance in microdissected collecting ducts: axial distribution and control by AVP. *Am J Physiol Renal Fluid Electrolyte Physiol* 271, F61-F70.

Kishore BK, Krane CM, Miller RL, Shi H, Zhang P, Hemmert A, Sun R & Nelson RD (2005). P2Y2 receptor mRNA and protein expression is altered in inner medullas of hydrated and dehydrated rats: relevance to AVP-independent regulation of IMCD function. *Am J Physiol Renal Physiol* 288, F1164-F1172.

Lolait SJ, O'Carroll AM, McBride OW, Konig M, Morel A & Brownstein MJ (1992). Cloning and characterization of a vasopressin V_2 receptor and possible link to nephrogenic diabetes insipidus. *Nature* 357, 336-339.

Machida K, Nonoguchi H, Wakamatsu S, Inoue H, Yosifovska T, Inoue T & Tomita K (2003). Acute regulation of the epithelial sodium channel gene by vasopressin and hyperosmolality. *Hypertens Res* 26, 629-634.

McKie AT, Powrie W & Naftalin RJ (1990). Mechanical aspects of fecal dehydration. *Am J Physiol* 258, G391-G394.

Mobasheri A, Wray S & Marples D (2005). Distribution of AQP2 and AQP3 water channels in human tissue microarrays. *J Mol Histol* 36, 1-14.

Morel A, O'Carroll AM, Brownstein MJ & Lolait SJ (1992). Molecular cloning and expression of a rat V_{1a} arginine vasopressin receptor. *Nature* 356, 523-526.

Moretó M, Cristià E, Pérez-Bosque A, Afzal-Ahmed I, Amat C & Naftalin RJ (2005). Aldosterone reduces crypt colon permeability during low-sodium adaptation. *J Membrane Biol* 206, 43-51.

Naftalin RJ & Pedley KC (1999). Regional crypt function in rat large intestine in relation to fluid absorption and growth of the pericryptal sheath. *J Physiol* 514, 211-227.

Naftalin RJ, Zammit PS & Pedley KC (1999). Regional differences in rat large intestinal crypt function in relation to dehydrating capacity in vivo. *J Physiol* 514, 201-210.

Naftalin RJ (2004). Alterations in colonic barrier function caused by a low sodium diet or ionizing radiation. *J Environ Pathol Toxicol Oncol* 23, 79-97.

Nagai Y, Miyata K, Sun GP, Rahman M, Kimura S, Miyatake A, Kiyomoto H, Kohno M, Abe Y, Yoshizumi M & Nishiyama A (2005). Aldosterone stimulates collagen gene expression and synthesis via activation of ERK1/2 in rat renal fibroblasts. *Hypertension* 46, 1039-1045.

Nicco C, Wittner M, DiStefano A, Jounier S, Bankir L & Bouby N (2001). Chronic exposure to vasopressin upregulates ENaC and sodium transport in the rat renal collecting duct and lung. *Hypertension* 38, 1143-1149.

Nielsen S, Chou CL, Marples D, Christensen EI, Kishore BK & Knepper MA (1995). Vasopressin increases water permeability of kidney collecting duct by inducing translocation of aquaporin-CD water channels to plasma membrane. *Proc Natl Acad Sci USA* 92, 1013-1017.

Noda Y & Sasaki S (2005). Trafficking mechanism of water channel aquaporin-2. *Biol Cell* 97, 885-892.

Nonoguchi H, Sands JM & Knepper MA (1988). Atrial natriuretic factor inhibits vasopressin-stimulated osmotic water permeability in rat inner medullary collecting duct. *J Clin Invest* 82, 1383-1390.

Nonoguchi H, Owada A, Kobayashi N, Takayama M, Terada Y, Koike J, Ujiie K, Marumo F, Sakai T & Tomita K (1995). Immunohistochemical localization of V2 vasopressin receptor along the nephron and functional role of luminal V2 receptor in terminal inner medullary collecting ducts. *J Clin Invest* 96, 1768-1778.

Roberts AB, Sporn MB, Assoian RK, Smith JM, Roche NS, Wakefield LM, Heine UI, Liotta LA, Falanga V, Kehrl JH & Fauci AS (1986). Transforming growth factor type β: rapid induction of fibrosis and angiogenesis in vivo and stimulation of collagen formation in vitro. *Proc Natl Acad Sci USA* 83, 4167-4171.

Sanghi P, Uretsky BF & Schwarz ER (2005). Vasopressin antagonism: a future treatment option in heart failure. *Eur Heart J* 26, 538-543.

Saito T, Ishikawa SE, Sasaki S, Fujita N, Fushimi K, Okada K, Takeuchi K, Sakamoto A, Ookawara S, Kaneko T & Marumo F (1997). Alteration in water channel AQP2 by removal of AVP stimulation in collecting duct cells of dehydrated rats. *Am J Physiol Renal Physiol* 272, F183-F191.

Sato Y, Hanai H, Nogaki A, Hirasawa K, Kaneko E, Hayashi H & Suzuki Y (1999). Role of the vasopressin V(1) receptor in regulating the epithelial functions of the guinea pig distal colon. *Am J Physiol* 277, G819-G828.

Schafer JA & Hawk CT (1992). Regulation of Na^+ channels in the cortical collecting duct by AVP and mineralcorticoids. *Kidney Int* 41, 255-268.

Stokes JB & Sigmund RD (1998). Regulation of rENaC mRNA by dietary NaCl and steroids: organ, tissue and steroid heterogeneity. *Am J Physiol* 274, C1699-C1707.

Szalay KSz, Beck M, Toth M & de Chatel R (1998). Interactions between ouabain, atrial natriuretic peptide, angiotensin II and potassium: effects on rat zona glomerulosa aldosterone production. *Life Sci* 62, 1845-1852.

Tahara A, Tomura Y, Wada K, Kusayama T, Tsukada J, Ishii N, Yatsu T, Uchida W & Tanaka A (1998). Effect of YM087, a potent nonpeptide vasopressin antagonist, on vasopressin-induced protein synthesis in neonatal rat cardiomyocyte. *Cardiovasc Res* 38, 198-205.

Taylor MM & Samson WK (2002). Adrenomedullin and the integrative physiology of fluid and electrolyte balance. *Microsc Res Tech* 57, 105-109.

Terris J, Ecelbarger CA, Nielsen S & Knepper MA (1996). Long-term regulation of four renal aquaporins in rats. *Am J Physiol Renal Fluid Electrolyte Physiol* 271, F414-F422.

Thiagarajah JR, Jayaraman S, Naftalin RJ, Verkman AS (2001a). In vivo fluorescence measurement of Na^+ concentration in the pericryptal space of mouse descending colon. *Am J Physiol* 281, C1898-C1903.

Thiagarajah JR, Pedley KC & Naftalin RJ (2001b). Evidence of amiloride-sensitive fluid absorption in rat descending colonic crypts from fluorescence recovery of FITC-labeled dextran after photobleaching. *J Physiol* 536, 541-553.

Thiagarajah JR, Griffiths NM, Pedley KC & Naftalin RJ (2002). Evidence for modulation of pericryptal sheath myofibroblasts in rat descending colon by transforming growth factor beta and angiotensin. *BMC Gastroenterol* 2, 4-15.

Verrey F (1994). Antidiuretic hormone action in A6 cells: effect on apical Cl and Na conductances and synergism with aldosterone for NaCl reabsorption. *J Membr Biol* 138, 65-76.

Yamamura Y, Nakamura S, Itoh S, Hirano T, Onogawa T, Yamashita T, Yamada Y, Tsujimae K, Aoyama M, Kotosai K, Ogawa H, Yamashita H, Kondo K, Tominaga M, Tsujimoto G & Mori T (1998). OPC-41061, a highly potent human vasopressin V2-receptor antagonist: pharmacological profile and aquaretic effect by single and multiple oral doping in rats. *J Pharmacol Exp Ther* 287, 860-867.

Zammit PS, Mendizabal M & Naftalin RJ (1994). Effects on fluid and Na^+ flux of varying luminal hydraulic resistance in rat colon in vivo. *J Physiol* 477, 539-548.

Zannad F & Radauceanu A (2005). Effect of MR blockade on collagen formation and cardiovascular disease with a specific emphasis on heart failure. *Heart Fail Rev* 10, 71-78.

Acknowledgements

This work was supported by projects BFI2003-05124 (Ministerio de Ciencia y Tecnología, Spain) and 2005SGR00632 (Generalitat de Catalunya, Spain). Esther Cristià was recipient of a FPU grant from MEC (Spain). We are grateful to Otsuka Pharmaceutical Co. (Japan) for the gift of Tolvaptan and to Dr. Carme Villà for plasma ion determinations. The support of the Confocal Service and the ICP-OES Service, Serveis Científicotècnics, Universitat de Barcelona are also acknowledged.